ZBP1/DAI is an innate sensor of influenza virus triggering the NLRP3 inflammasome and programmed cell death pathways

Teneema Kuriakose[1], Si Ming Man[1], R.K. Subbarao Malireddi[1], Rajendra Karki[1], Sannula Kesavardhana[1], David E. Place[1], Geoffrey Neale[2], Peter Vogel[3], and Thirumala-Devi Kanneganti[1]*

[1] Department of Immunology, St. Jude Children's Research Hospital, Memphis, TN, 38105, USA;

[2] Hartwell Center for Bioinformatics & Biotechnology, St. Jude Children's Research Hospital, Memphis, TN, 38105, USA;

[3] Animal Resources Center and the Veterinary Pathology Core, St. Jude Children's Research Hospital, Memphis, TN, 38105, USA.

*Correspondence to:

Thirumala-Devi Kanneganti

Department of Immunology, St. Jude Children's Research Hospital

MS #351, 262 Danny Thomas Place

Memphis TN 38105-3678

Tel: (901) 595-3634; Fax. (901) 595-5766.

E-mail: Thirumala-Devi.Kanneganti@StJude.org

One sentence summary: ZBP1 activates the NLRP3 inflammasome and programmed cell death.

Keywords: ZBP1, DAI, NLRP3, inflammasome, caspase-1, pyroptosis, necroptosis, apoptosis, influenza virus, IFNs, caspase-8, RIPK3.

ABSTRACT

Z-DNA binding protein 1 (ZBP1, also known as DNA-dependent activator of IFN-regulatory factors (DAI) and DLM-1) was identified as a dsDNA sensor, which instigates innate immune responses. However, this classification has been disputed and whether ZBP1 functions as a pathogen sensor during an infection has remained unknown. Herein, we demonstrated ZBP1-mediated sensing of the influenza A virus (IAV) proteins NP and PB1, triggering either cell death or inflammatory responses via components of the RIPK1–RIPK3–Caspase-8 axis. ZBP1 regulates NLRP3 inflammasome activation as well as induction of apoptosis, necroptosis and pyroptosis in IAV-infected cells. Importantly, ZBP1 deficiency protected mice from mortality during IAV infection owing to reduced inflammatory responses and epithelial damage. Overall, these findings indicate that ZBP1 is an innate immune sensor of IAV and highlight its importance in the pathogenesis of IAV infection.

INTRODUCTION

The influenza virus infects millions of people annually and causes significant morbidity and up to half a million deaths (*1*). Type A Influenza virus (IAV) is also associated with epidemics and pandemics owing to high mutation rates and genetic reassortment. Pattern-recognition receptors, including Toll-like receptors (TLRs), RIG-I-like receptors (RLRs) and nucleotide and oligomerization domain, leucine-rich repeats-containing proteins (NLRs) have a central role in the recognition of IAV infection (*2*). Virus sensing by these receptors initiates an innate immune response aimed at controlling virus replication and eliminating the infectious virus.

Innate sensing of IAV triggers multiple intracellular signaling cascades that coordinately regulate induction of type I interferon (IFNs) and proinflammatory cytokines (*2*). In addition, virus sensing also induces cell death in order to destroy the replicative niche necessary for survival and propagation of these intracellular pathogens (*3*). While epithelial cell death facilitates control of virus replication by eliminating infected cells, uncontrolled cell death can exacerbate tissue injury and compromise lung function (*4*). Previous studies have demonstrated an inherent link between orchestration of various programmed cell death pathways and pathogenesis of IAV (*5*). Consistent with this, apoptosis in lung epithelial cells was shown to exacerbate pneumonia and mortality during IAV infection (*6*). Similarly, uncontrolled necroptosis in airway epithelial cells also increases morbidity and mortality during IAV infection (*7*). Unlike the detrimental effects of apoptosis and necroptosis, NLRP3 inflammasome activation leading to pyroptosis and release of proinflammatory cytokines IL-1β and IL-18 is protective during acute IAV infection (*8, 9*). Although all these cell death pathways are known to be activated during IAV infection, the innate immune sensors initiating cell death and the intracellular

signaling cascades defining this response are largely unknown and are explored in this study.

RESULTS

The IFN-inducible protein ZBP1 mediates cell death in response to IAV infection.

To delineate the virus sensing pathways initiating cell death responses during IAV infection, cell death was assessed in primary murine BMDMs infected with Influenza virus A/Puerto Rico/8/34 (PR8; H1N1). BMDMs lacking the TLR adaptor proteins MyD88 or TRIF, or the RIG-I adaptor MAVS undergo cell death during infection with this mouse-adapted virus, probably due to functional redundancy of TLR and RIG-I pathways in IAV sensing in these cells (*2*) (**fig. S1A to C)**. BMDMs and fibroblasts lacking the adaptor STING, TNF receptor 1 (TNFR1), TNFR2 or the adaptor molecule TNFR1-associated death domain protein (TRADD) were also susceptible to IAV-induced cell death (**Fig. 1A to D and fig. S1B to C**). In contrast, cells lacking type I IFN receptor 1 (IFNAR1) or its downstream signaling proteins STAT1 and IRF9 were fully resistant to IAV-induced cell death (**Fig. 1A to D and fig. S1D**). Increased levels of IAV M1 and NS1 proteins confirmed proper virus entry and replication in these cells (**fig. S1E**). These results demonstrated that cell death during IAV infection is initiated through a pathway mediated by type I IFN signaling.

Enrichment of the microarray gene expression dataset from IAV-infected WT and *Ifnar1*$^{-/-}$ BMDMs for nucleic acid sensing pathways followed by qRT-PCR revealed a significant reduction in the expression of a number of genes encoding proinflammatory cytokines and nucleic acid sensors in *Ifnar1*$^{-/-}$ BMDMs compared to WT BMDMs (**Fig. 1E to F and fig. S2A**). Interestingly, one of the most down-regulated nucleic acid sensors in *Ifnar1*$^{-/-}$ BMDMs was the gene encoding Z–□□□ binding protein 1 (ZBP1; also called DLM-1 and DAI) (**Fig. 1E to F**). Expression of ZBP1 was robustly upregulated in WT BMDMs infected with IAV, through a mechanism that required IFNAR1, STAT1 and IRF9 (**Fig. 1G to H and fig. S2B**). ZBP1 was initially identified as a cytosolic sensor of double-stranded (ds)DNA which drives type I IFN responses (*10*). ZBP1 was of potential interest

because of its disputed role in cytosolic DNA sensing after generation of *Zbp1*$^{-/-}$ mice (*11-13*), however, it may have a role in regulation of cell death during infection with a mutant form of the DNA virus murine cytomegalovirus (MCMV) (*10-14*).

The IFNAR-dependent cell death observed in IAV-infected cells prompted us to hypothesize that ZBP1 is a cytosolic sensor of IAV driving cell death responses. Remarkably, *Zbp1*$^{-/-}$ BMDMs and fibroblasts were completely resistant to IAV-induced cell death (**Fig. 1I to L**). Real time analysis of ZBP1-dependent cell death in IAV-infected fibroblasts using IncuCyte and SYTOX green nucleic acid staining demonstrated that cell death was initiated at 8 to 10 h post infection (pi) which corresponds to one replication cycle of IAV (**Fig. 1M**). Comparable levels of the viral protein NS1 and IFNβ in *Zbp1*$^{-/-}$ BMDMs infected with IAV confirmed proper virus entry and replication and IFNβ secretion in these cells (**fig. S2C to D).** Together, these data demonstrate a critical role for ZBP1 in the regulation of cell death during IAV infection.

ZBP1 regulates NLRP3 inflammasome activation and proinflammatory cytokine production during IAV infection via the RIPK1–RIPK3–Caspase-8 axis.

Distinct forms of programmed cell death, including pyroptosis, necroptosis and apoptosis, are initiated by context-specific stimuli encountered by the cell (*15*). Previous studies have demonstrated NLRP3 inflammasome-mediated activation of the pyroptosis-inducing cysteine protease, caspase-1, during IAV infection (*16-19*). While robust activation of caspase-1 was observed in WT BMDMs infected with IAV, this response was abrogated in *Zbp1*$^{-/-}$, *Ifnar1*$^{-/-}$ and *Nlrp3*$^{-/-}$ BMDMs (**Fig. 2A**). Furthermore, the levels of the inflammasome-dependent cytokines, IL-1β and IL-18, were significantly reduced in *Zbp1*$^{-/-}$ and *Ifnar1*$^{-/-}$ cells compared to WT BMDMs (**Fig. 2B to C**), confirming

a requirement for ZBP1 and type I IFN signaling in the activation of the NLRP3 inflammasome during IAV infection. ZBP1 was dispensable for the activation of caspase-1 and the release of IL-1β and IL-18 in response to the RNA virus vesicular stomatitis virus (VSV), the canonical NLRP3 activator LPS plus ATP, and to the non-canonical NLRP3 activators *Escherichia coli* and *Citrobacter rodentium* infection (**Fig. 2D and fig. S3A to C)**. Notably, NLRP3 inflammasome activation during IAV infection did not require caspase-11 (**Fig. 2E**). These data identified a unique, type I IFN- and ZBP1-dependent pathway of NLRP3 inflammasome activation, which differ from the canonical and non-canonical NLRP3 inflammasome pathways.

ZBP1 is dispensable for activation of the NLRC4 and AIM2 inflammasomes since infection by *Salmonella enterica* serovar Typhimurium, *Francisella novicida* and MCMV, as well as transfection of poly(dA:dT) induced normal caspase-1 activation and secretion of IL-1β or IL-18 in *Zbp1*$^{-/-}$ BMDMs (**fig. S3D to G**). Although ZBP1 is a key regulator of IAV-induced NLRP3 inflammasome activation, ZBP1-dependent cell death during IAV infection occurred normally in *Nlrp3*$^{-/-}$, *Casp1*$^{-/-}$ and *Gsdmd*$^{-/-}$ BMDMs (**fig. S4A to D**). These data suggest activation of other complimentary cell death pathways in IAV-infected cells.

ZBP1 contains two receptor-interacting protein homotypic interaction motif (RHIM) domains that can interact with other RHIM-containing proteins including the receptor interacting protein kinase-3 (RIPK3) (*20, 21*). Indeed, immunoprecipitation experiments revealed interaction of ZBP1 with RIPK3 in IAV-infected cells (**Fig. 2F**). Consistent with previous studies demonstrating RIPK3-mediated activation of the NLRP3 inflammasome (*19, 22, 23*), a substantial reduction in caspase-1 cleavage and the levels of IL-1β and IL-18 were observed in *Ripk3*$^{-/-}$ BMDMs infected with IAV (**Fig. 2G to H**). The residual activation of caspase-1 observed in *Ripk3*$^{-/-}$ BMDMs was abolished in *Ripk3*$^{-/-}$*Casp8*$^{-/-}$

BMDMs (**Fig. 2G**). BMDMs lacking RIPK1 kinase activity (*Ripk1*$^{KD/KD}$) showed normal activation of caspase-1 and release of IL-1β and IL-18 (**Fig. 2G to H**).

ZBP1-RIPK1 complex transduces NFκB activation signals (*20, 21*). Consistent with previous findings, secretion of proinflammatory cytokines, IL-6 and TNF were abrogated in *Ripk3*$^{-/-}$*Casp8*$^{-/-}$*Ripk1*$^{-/-}$ as well as *Zbp1*$^{-/-}$ BMDMs (**Fig. 2I to J)**. A modest reduction in IL-6 and TNF production was observed in *Ripk3*$^{-/-}$ and *Ripk3*$^{-/-}$*Casp8*$^{-/-}$ BMDMs (**Fig. 2I).** Regulation of IL-6 and TNF production is dependent on RIPK1 scaffolding function, but occurs independently of its kinase activity since the levels of these cytokines were comparable in WT and *Ripk1*$^{KD/KD}$ cells (**Fig. 2I**). Collectively, these data identified ZBP1 as an upstream regulator mediating NLRP3 inflammasome activation via the RIPK3–Caspase-8 axis and proinflammatory responses via RIPK1.

ZBP1 mediates RIPK3-dependent induction of apoptotic and necroptotic cell death pathways during IAV infection

Previous studies identified RIPK3 as a critical regulator determining cell death via necroptotic or apoptotic pathways (*24, 25*). BMDMs and fibroblasts lacking RIPK3 or both RIPK3 and caspase-8 or RIPK3 and FADD were fully resistant to IAV-induced cell death, confirming a critical role of RIPK3 in mediating ZBP1-dependent cell death (**Fig. 3A to C and fig. S5A**). Necroptosis is executed by the RIPK3 substrate mixed lineage kinase like (MLKL) (*26*). However, cell death comparable to WT levels was observed in *Mlkl*$^{-/-}$ BMDMs and fibroblasts infected with IAV, demonstrating that MLKL is dispensable for ZBP1- and RIPK3-dependent cell death (**Fig. 3A to C and fig. S5A**).

ZBP1 also controls apoptosis during IAV infection since activation of caspase-8, caspase-3 and caspase-7 were abrogated in *Zbp1*$^{-/-}$ BMDMs compared to WT BMDMs infected with IAV (**Fig. 3D)**. Robust activation of both caspase-1 and caspase-8 were observed in *Mlkl*$^{-/-}$ BMDMs infected with IAV and inhibition of these caspase activities

using zIETD-FMK (blocks both caspase-8 and caspase-1) prevented IAV-induced cell death in *Mlkl*$^{-/-}$ BMDMs (**Fig. 3E and fig. S5B to D)**. Activation of multiple, complementary cell death pathways in IAV-infected cells was further confirmed by simultaneous inhibition of apoptosis, pyroptosis and necroptosis in WT BMDMs with the caspase-8 inhibitor zIETD-FMK plus MLKL inhibitor GW806742X (*27*). Treatment with these inhibitors prevented WT BMDMs from undergoing cell death during IAV infection (**Fig. 3E**). Inhibition of either apoptosis or necroptosis in WT and *Casp1*$^{-/-}$ BMDMs was unable to block IAV-induced cell death (**Fig. 3E and fig. S5D**). These results collectively demonstrate parallel contribution of pyroptosis, necroptosis and apoptosis in the execution of IAV-induced cell death governed by ZBP1.

ZBP1 regulates cell death in response to both mouse-adapted and seasonal strains of IAV, but not in response to other RNA viruses.

In addition to mouse adapted PR8 virus, ZBP1 also regulates cell death in response to IAV of different species- and strain-specificity since *Zbp1*$^{-/-}$ fibroblasts were protected from cell death during infection with mouse adapted Influenza A/X31 (H3N2) as well as non-mouse adapted seasonal strains Influenza A/Brisbane/59/2007 (H1N1) and A/Switzerland/9715293/2013 (H3N2) (**Fig. 4A to F)**. Unlike different strains of IAV, cell death as well as inflammatory cytokine production occurred independently of ZBP1 in BMDMs infected with other negative sense RNA viruses, VSV, Sendai virus (SeV) and respiratory syncytial virus (RSV) (**Fig. 2D, Fig. 4G and fig. S6**). Moreover, transfection of synthetic, IAV or mammalian-derived ssRNA species as well as the dsRNA ligand poly(I:C) and dsDNA ligand poly(dA:dT) induced comparable levels of cell death in WT and *Zbp1*$^{-/-}$ BMDMs (**fig. S7A to C**). Together, these data highlighted an IAV-specific role for ZBP1 in initiating cell death responses.

ZBP1 is a sensor of IAV nucleoprotein (NP) and polymerase subunit PB1.

To investigate potential interaction of ZBP1 with IAV proteins, endogenous ZBP1 was immunoprecipitated from IAV-infected cells and probed for interacting IAV proteins. Immunoblotting for IAV M1, NS1 and HA proteins did not show any detectable levels of protein interaction (**Fig. 5A**). Interestingly, the IAV nucleoprotein (NP) and RNA polymerase subunit PB1 were co-precipitated from WT, but not *Zbp1*$^{-/-}$ fibroblasts infected with IAV (**Fig. 5B**). Conversely, immunoprecipitation of NP or PB1 from lysates of IAV-infected fibroblasts also showed co-precipitation of these proteins with ZBP1, confirming interaction of endogenous ZBP1 with NP and PB1 (**Fig. 5C**). ZBP1, PB1 and NP were observed in both nuclear and cytoplasmic fractions from infected cells at 8hr post infection indicating that ZBP1 interaction with viral proteins can occur in either or both of these compartments (**Fig. 5D**). Overexpression of PB1 or NP in ZBP1-expressing 293T cells also demonstrated interaction of these viral proteins with ZBP1 (**Fig. 5E**).

In order to map the domains with which ZBP1 interacts with IAV proteins, various deletion mutants of ZBP1 with HA tag was generated and overexpressed in 293T cells (**Fig. 5F**). Efficient co-immunoprecipitation of PB1 or NP proteins with WT ZBP1 and ZBP1 lacking the RHIM, but not with ZBP1 lacking the C-terminal domain, demonstrated the importance of the C-terminal domain of ZBP1 for its interaction with IAV proteins (**Fig. 5G to H**). In addition to C-terminal domain, the Zα domain of ZBP1 was also required for interaction with PB1 (**Fig. 5G**). Collectively, we identified ZBP1 as a sensor of influenza virus proteins and can trigger both cell death and inflammatory responses during infection.

ZBP1 promotes inflammatory responses and epithelial damage during IAV infection *in vivo.*

The physiological relevance of ZBP1 in regulating pathogenesis of IAV infection was assessed in WT and *Zbp1*$^{-/-}$ mice infected with one LD_{50} of PR8 virus. Remarkably, *Zbp1*$^{-/-}$ mice were protected from mortality during IAV infection (**Fig. 6A**). These mice also showed a significant reduction in weight loss and morbidity during the early phase of infection compared to WT mice (**Fig. 6B**). However, viral titers were significantly higher in *Zbp1*$^{-/-}$ mice at day 7 pi consistent with the notion that cell death destroys the niche necessary for virus replication (**Fig. 6C**). The defective viral clearance observed in *Zbp1*$^{-/-}$ mice led to increased weight loss at later stages of infection and these mice showed delayed recovery from infection compared to WT animals (**Fig. 6B**). In agreement with our *in vitro* findings, inflammatory responses as well as epithelial damage was markedly reduced in *Zbp1*$^{-/-}$ mice infected with IAV (**Fig. 6D to E**). While severe and extensive inflammatory responses characterized by diffuse intra-alveolar infiltrates of neutrophils and macrophages and perivascular accumulations of lymphocytes and granulocytes were observed in the lungs of WT mice, these responses were reduced in *Zbp1*$^{-/-}$ mice on day 7 pi (**Fig. 6D**). Collectively, these data demonstrated a critical role of ZBP1 in regulating pathogenesis and immunopathology during acute IAV infection by controlling both cell death and inflammatory responses.

DISCUSSION

Cell fate decisions are well integrated into antiviral immune responses during an infection and are critical for elimination of replicating viruses. Although cell death constitutes a major antiviral host defense mechanism during IAV infection, exaggerated responses often leads to severe clinical disease and mortality as exemplified by the substantial damage to the lungs and destruction of respiratory epithelium observed in autopsy samples from the 1918 influenza pandemic (*28*). Despite the importance of epithelial cell death in determining disease outcome during acute IAV infection, the host factors regulating cell death responses are less characterized.

The critical role of type I IFN signaling in potentiating IAV-induced apoptosis in MEFs via activation of the FADD–caspase-8 signaling axis has been reported (*29*). Induction of IFNAR1–RIPK3-dependent necroptosis was also demonstrated in both MEFs and macrophages when FADD–caspase-8 signaling was inactivated (*30, 31*). Although ISGF3 complex was recognized as a critical promoter of necroptosis, the IFN-stimulated gene mediating necroptosis and inflammatory responses in macrophages is not identified so far (*31*). In addition to these *in vitro* studies, pathogenic potential of type I IFN signaling in mediating uncontrolled inflammatory response and epithelial cell death was also demonstrated during IAV infection *in vivo* (*32*). Our study now identified ZBP1 as the IFN-inducible protein regulating both inflammatory responses and cell death during IAV infection *in vitro* and *in vivo*.

The RHIM domains of ZBP1 associate with RHIM domains of both RIPK1 and RIPK3 to mediate NFκB activation and cell death responses (*14, 20, 21*). Consistent with these findings, we observed a critical role for ZBP1–RIPK1 axis in mediating proinflammatory responses during IAV infection. Moreover, ZBP1 regulation of cell death in IAV-infected cells is mediated via RIPK3. Of note, while our manuscript was in revision Nogusa et al.

reported RIPK3-dependent activation of parallel necroptotic and apoptotic pathways in IAV-infected cells (*33*). Although this study demonstrate the importance of RIPK3 in driving cell death during IAV-infection, the upstream receptors and signaling pathways regulating RIPK3 was not identified.

Despite being identified as a DNA sensor, it is still unclear whether ZBP1 functions as a pathogen sensor during an infection. Our study now identified ZBP1 for the recognition of an RNA virus, and in particular linking it to both immune and cell death responses to clinically relevant IAV infection. Innate sensors of IAV have been well characterized, however all known IAV-receptors recognize viral nucleic acids in infected cells (*2*). Notably, our study demonstrates ZBP1 as an innate receptor of IAV proteins regulating antiviral innate immune responses.

After our discovery of IAV-induced NLRP3 inflammasome activation almost a decade ago (*16*), multiple studies have investigated the molecular and cellular mechanisms regulating inflammasome assembly in response to IAV infection (*17-19, 34-36*). The importance of IAV M2 ion channel protein, RIG-I, type I IFN signaling, RIPK3 and RNaseL in mediating inflammasome activation during IAV infection have been demonstrated (*18, 19, 34, 36*). Our data demonstrating an IAV-specific role for IFNAR–ZBP1 axis in the regulation of NLRP3 inflammasome activation will help to reconcile these findings. While both RIG-I and RNaseL mediates type I IFN production which is necessary for induction of ZBP1, RIPK3 associates with ZBP1 to transduce downstream signals. The interconnected and complimentary nature of IAV-induced cell death pathways demonstrated in our study also helps to explain PB1-F2-mediated NLRP3 inflammasome activation since PB1-F2 is regarded as the viral effector mediating cell death in IAV-infected cells (*35, 37*). Therefore, the identification of ZBP1 as an IAV-specific sensor helps to further resolve the molecular mechanisms regulating NLRP3 inflammasome assembly during IAV infection.

The seemingly paradoxical observations of reduced mortality in *Zbp1*$^{-/-}$ mice in spite of increased viral titers are not unexpected, since previous studies in both humans and animal models reported exaggerated inflammatory response, substantial loss of pulmonary epithelia and acute lung injury as the major factors contributing to morbidity and mortality during pathogenic IAV infection (*38, 39*). An extensive systems analysis study also demonstrated elevated activation of inflammatory signaling networks as a signature that distinguishes lethal from sublethal IAV infections (*40*). Moreover, transcriptome analysis of lung samples from infected mice identified immune and cell death responses as the major factor distinguishing mild from highly pathogenic infections (*41*). Our data are in agreement with these studies demonstrating exaggerated immune response rather than direct viral damage as the key trigger potentiating mortality during IAV infection.

Although BMDMs and fibroblasts do not represent the major cell types infected during IAV infection, the *in vitro* data obtained from these cells are validated by *in vivo* infections. However, further studies are warranted to identify the host and viral effectors as well as the precise molecular mechanism by which ZBP1-dependent cell death is executed in IAV-infected cells. The relevance of human ZBP1 during IAV infection was also not assessed in our study. *In vitro* studies investigating the role of human ZBP1 during IAV infection are less feasible since most of the lung epithelial cell lines that support productive virus replication do not undergo IAV-induced cell death (*37*). Notably, proteomics analysis of human innate immunity interactome for type I IFN identified ZBP1 as one of the interacting proteins with antiviral activity (*42*). Moreover, human ZBP1 restricts replication of both human cytomegalovirus and herpes simplex-1 demonstrating functional importance of ZBP1 in antiviral responses (*43, 44*). Since cell death, inflammatory responses and virus replication are intricately associated with each other, various host factors modulating susceptibility to infection as well as dosage of infection

will be critical in determining the role of ZBP1 in disease progression. Identification of genetic lesions in *ZBP1* locus in patient populations will be of great value and further studies in this direction are necessary to determine the importance of ZBP1 in pathogenesis of IAV in humans. Nevertheless, the insights gained from this study improve our understanding about the mechanisms regulating pathogenesis and prognosis of acute influenza virus infection and may lead to improved disease intervention strategies for the prevention and treatment of IAV infection.

Materials and Methods:

Study Design

Animal studies were conducted under protocols approved by the St. Jude Children's Research Hospital on the Use and Care of Animals. Age- and sex-matched, 6- to 8-week-old WT *and* *Zbp1*$^{-/-}$ mice (at least five animals per group) bred at the Animal Research Center at SJCRH were used for *in vivo* experiments. Infected mice were monitored and body weights were recorded daily, and mice exhibiting severe signs of disease or more than 30% weight loss relative to pre-infection body weight were euthanized. Animals were euthanized at indicated time points for lung harvest. Lung sections were processed at Veterinary Pathology Core at SJCRH and histopathological analysis was conducted by a pathologist blinded to experimental groups.

Mice

Zbp1$^{-/-}$, *Ifnar1*$^{-/-}$, *Stat1*$^{-/-}$, *Irf9*$^{-/-}$, *Aim2*$^{-/-}$, *Nlrp3*$^{-/-}$, *Nlrc4*$^{-/-}$, *Casp1*$^{-/-}$, *Casp11*$^{-/-}$, *Mavs*$^{-/-}$, *Myd88*$^{-/-}$, *Trif*$^{-/-}$, *Tradd*$^{-/-}$, *Sting*$^{Gt/Gt}$, *Ripk3*$^{-/-}$, *Ripk3*$^{-/-}$*Casp8*$^{-/-}$, *Ripk3*$^{-/-}$*Casp8*$^{-/-}$*Ripk1*$^{-/-}$, *Ripk1*$^{KD/KD}$ and *Mlkl*$^{-/-}$ mice have been described previously (*13, 45-48*). *Tnfr*$^{-/-}$ mice (Stock #003243) were purchased from The Jackson Laboratory.

Cell culture and stimulation

Cells were cultured overnight in antibiotic–free media before infection. The influenza A/Puerto Rico/8/34 virus (PR8) generated by an eight-plasmid reverse genetics system was propagated in allantoic cavity of 9- to 11-day-old embryonated SPF chicken eggs and viral titers were enumerated by plaque assays. BMDMs (MOI, 25) and fibroblasts (MOI, 10) were infected with PR8 virus for 2 h. DMEM media containing 20% FBS was added after 2 h and samples were collected at indicated time points. For

pharmacological inhibition, BMDMs treated with 5 □M Z-VAD-FMK (Calbiochem) and/or 1□M GW806742X (SYNkinase) at the same time as IAV infection. RSV Line 19F was grown in HEp-2 cell line.

Microarray analysis

RNA was extracted from BMDMs infected with PR8 virus 9h pi (MOI, 25) using TRIzol according to the manufacturer's instructions (Life Technologies). Transcript profiling was performed using two biological replicate samples. Total RNA (100 ng) was converted to biotin-labeled cRNA using the Ambion WT expression kit (Life Technologies) and hybridized to a Mouse Gene 2.0 ST GeneChip (Affymetrix, Inc). After staining and washing, array signals were normalized and transformed into $\log_2$ transcript expression values using the Robust Multi-array Average algorithm (Partek Genomics Suite v6.6). Differential expression was defined by applying a 0.5 $\log_2$(signal) difference between conditions. Lists of differentially expressed transcripts were analyzed for functional enrichment using the DAVID bioinformatics databases (http://david.abcc.ncifcrf.gov/) and Ingenuity Pathways Analysis software (www.qiagen.com/ingenuity).

Cytokine measurement

IFNβ and IL-18 was measured using an ELISA kit (BioLegend (IFNβ); eBioscience (IL-18)). All other cytokines were measured by multiplex ELISAs (Millipore).

Immunoblotting analysis

For caspase-1 immunoblotting, BMDMs and supernatant were lysed in cell lysis buffer. For immunoblotting other proteins, cells were lysed in RIPA buffer and sample loading buffer containing SDS and 100 mM DTT after washing with cold PBS. Proteins were separated on 8-12% polyacrylamide gels and transferred onto PVDF membranes.

Membranes were blocked in 5% skim milk followed by incubation with primary antibodies and secondary HRP antibodies. The details of antibodies used are given in supplementary materials.

Generation of ZBP1 overexpressing cells

pVSVg, pEQ-Pam3(-E) and pMIGII plasmids encoding the *Zbp1* gene are transfected into 293T cells to generate retroviral stocks. Retroviral supernatants were harvested after 48 hours of transfection and filtered through 0.4uM sterile filters. 293T cells were infected with the corresponding retroviral stocks in the presence of polybrene to generate cells stably expressing the respective ZBP1 proteins.

Co-immunoprecipitation

For immunoprecipitation, cell lysates were incubated with 3 µg of indicated primary antibodies on a rocking platform for 12-16h at 4°C. Protein A/G PLUS-Agarose (Santa Cruz) was added to the samples and incubated for another 2 h on the rocking platform. Agarose was centrifuged and washed 3 times with the lysis buffer. Immunoprecipitates were eluted in sample buffer after three washes in lysis buffer and then subjected to immunoblotting analysis.

Animal infection

WT *and* *Zbp1*$^{-/-}$ mice were anesthetized with 250 mg/kg Avertin followed by intranasal infection with one LD_{50} of PR8 virus in 30 µl PBS. Infected mice were observed over a period of 18 days for survival study. Lungs were harvested on day 7 pi and left lobe of the lungs was used for histopathological analysis. Formalin-preserved lungs were processed and embedded in paraffin according to standard procedures. Sections were

stained with hematoxylin and eosin (H&E) or IAV nucleoprotein. Lung viral titers were enumerated by plaque assays after homogenizing lungs in 1 ml PBS using a bead mill homogenizer (Qiagen).

Statistical analysis

GraphPad Prism 6.0 software was used for data analysis. Statistical significance was determined by a paired two-tailed *t* test or one-way ANOVA; $P < 0.05$ was considered statistically significant where $*P<0.05$, $**P<0.01$, and $***P<0.001$. Mean ± sem of the data is presented.

List of supplementary materials:

1. **Materials and methods**
2. **Fig. S1:** Cell death induced by IAV infection in BMDMs occurs independently of MyD88, MAVS, TRIF, STING and TRADD, but is dependent on the transcription factors STAT1 and IRF9.
3. **Fig. S2:** ZBP1 induced via IFN signaling regulates cell death in IAV-infected cells independently of virus replication and IFNβ production.
4. **Fig. S3:** ZBP1 is dispensable for activation of canonical and non-canonical NLRP3, NLRC4 and AIM2 inflammasomes.
5. **Fig. S4:** IAV-induced cell death is not prevented by the absence of the NLRP3, caspase-1 or gasdermin D.
6. **Fig. S5:** ZBP1 drives activation of complementary cell death pathways during IAV infection.

7. **Fig. S6:** ZBP1 is dispensable for proinflammatory cytokine production in response to other RNA viruses.
8. **Fig. S7:** ZBP1 is dispensable for cell death in response to transfected RNA and ds(DNA) ligands.
9. **Table S1:** Real-time qPCR primer sequences

References:

1. WHO. Influenza (Seasonal) Fact sheet N^0 211 2009 [updated April 2009; cited 2012 June 12, 2012]. Available from: http://www.who.int/mediacentre/factsheets/fs211/en/index.html.
2. A. Iwasaki, P. S. Pillai, Innate immunity to influenza virus infection. *Nature reviews. Immunology* **14**, 315-328 (2014); published online EpubMay (10.1038/nri3665).
3. I. Jorgensen, E. A. Miao, Pyroptotic cell death defends against intracellular pathogens. *Immunological reviews* **265**, 130-142 (2015); published online EpubMay (10.1111/imr.12287).
4. C. J. Sanders, P. Vogel, J. L. McClaren, R. Bajracharya, P. C. Doherty, P. G. Thomas, Compromised respiratory function in lethal influenza infection is characterized by the depletion of type I alveolar epithelial cells beyond threshold levels. *American journal of physiology. Lung cellular and molecular physiology* **304**, L481-488 (2013); published online EpubApr 1 (10.1152/ajplung.00343.2012).
5. S. Herold, S. Ludwig, S. Pleschka, T. Wolff, Apoptosis signaling in influenza virus propagation, innate host defense, and lung injury. *Journal of leukocyte biology* **92**, 75-82 (2012); published online EpubJul (10.1189/jlb.1011530).
6. S. Herold, T. S. Tabar, H. Janssen, K. Hoegner, M. Cabanski, P. Lewe-Schlosser, J. Albrecht, F. Driever, I. Vadasz, W. Seeger, M. Steinmueller, J. Lohmeyer, Exudate macrophages attenuate lung injury by the release of IL-1 receptor antagonist in gram-negative pneumonia. *American journal of respiratory and critical care medicine* **183**, 1380-1390 (2011); published online EpubMay 15 (10.1164/rccm.201009-1431OC).

7. I. G. Rodrigue-Gervais, K. Labbe, M. Dagenais, J. Dupaul-Chicoine, C. Champagne, A. Morizot, A. Skeldon, E. L. Brincks, S. M. Vidal, T. S. Griffith, M. Saleh, Cellular inhibitor of apoptosis protein cIAP2 protects against pulmonary tissue necrosis during influenza virus infection to promote host survival. *Cell host & microbe* **15**, 23-35 (2014); published online EpubJan 15 (10.1016/j.chom.2013.12.003).

8. P. G. Thomas, P. Dash, J. R. Aldridge, Jr., A. H. Ellebedy, C. Reynolds, A. J. Funk, W. J. Martin, M. Lamkanfi, R. J. Webby, K. L. Boyd, P. C. Doherty, T. D. Kanneganti, The intracellular sensor NLRP3 mediates key innate and healing responses to influenza A virus via the regulation of caspase-1. *Immunity* **30**, 566-575 (2009); published online EpubApr 17 (10.1016/j.immuni.2009.02.006).

9. I. C. Allen, M. A. Scull, C. B. Moore, E. K. Holl, E. McElvania-TeKippe, D. J. Taxman, E. H. Guthrie, R. J. Pickles, J. P. Ting, The NLRP3 inflammasome mediates in vivo innate immunity to influenza A virus through recognition of viral RNA. *Immunity* **30**, 556-565 (2009); published online EpubApr 17 (S1074-7613(09)00139-3 [pii]10.1016/j.immuni.2009.02.005).

10. A. Takaoka, Z. Wang, M. K. Choi, H. Yanai, H. Negishi, T. Ban, Y. Lu, M. Miyagishi, T. Kodama, K. Honda, Y. Ohba, T. Taniguchi, DAI (DLM-1/ZBP1) is a cytosolic DNA sensor and an activator of innate immune response. *Nature* **448**, 501-505 (2007); published online EpubJul 26 (10.1038/nature06013).

11. T. Schwartz, J. Behlke, K. Lowenhaupt, U. Heinemann, A. Rich, Structure of the DLM-1-Z-DNA complex reveals a conserved family of Z-DNA-binding proteins. *Nature structural biology* **8**, 761-765 (2001); published online EpubSep (10.1038/nsb0901-761).

12. Z. Wang, M. K. Choi, T. Ban, H. Yanai, H. Negishi, Y. Lu, T. Tamura, A. Takaoka, K. Nishikura, T. Taniguchi, Regulation of innate immune responses by

DAI (DLM-1/ZBP1) and other DNA-sensing molecules. *Proceedings of the National Academy of Sciences of the United States of America* **105**, 5477-5482 (2008); published online EpubApr 8 (10.1073/pnas.0801295105).

13. K. J. Ishii, T. Kawagoe, S. Koyama, K. Matsui, H. Kumar, T. Kawai, S. Uematsu, O. Takeuchi, F. Takeshita, C. Coban, S. Akira, TANK-binding kinase-1 delineates innate and adaptive immune responses to DNA vaccines. *Nature* **451**, 725-729 (2008); published online EpubFeb 7 (10.1038/nature06537).
14. J. W. Upton, W. J. Kaiser, E. S. Mocarski, DAI/ZBP1/DLM-1 complexes with RIP3 to mediate virus-induced programmed necrosis that is targeted by murine cytomegalovirus vIRA. *Cell host & microbe* **11**, 290-297 (2012); published online EpubMar 15 (10.1016/j.chom.2012.01.016).
15. S. M. Man, T. D. Kanneganti, Converging roles of caspases in inflammasome activation, cell death and innate immunity. *Nature reviews. Immunology* **16**, 7-21 (2016); published online EpubJan (10.1038/nri.2015.7).
16. T. D. Kanneganti, M. Body-Malapel, A. Amer, J. H. Park, J. Whitfield, L. Franchi, Z. F. Taraporewala, D. Miller, J. T. Patton, N. Inohara, G. Nunez, Critical role for Cryopyrin/Nalp3 in activation of caspase-1 in response to viral infection and double-stranded RNA. *The Journal of biological chemistry* **281**, 36560-36568 (2006); published online EpubDec 1 (10.1074/jbc.M607594200).
17. T. Ichinohe, H. K. Lee, Y. Ogura, R. Flavell, A. Iwasaki, Inflammasome recognition of influenza virus is essential for adaptive immune responses. *J Exp Med* **206**, 79-87 (2009); published online EpubJan 16 (jem.20081667 [pii]10.1084/jem.20081667).
18. T. Ichinohe, I. K. Pang, A. Iwasaki, Influenza virus activates inflammasomes via its intracellular M2 ion channel. *Nature immunology* **11**, 404-410 (2010); published online EpubMay (10.1038/ni.1861).

19. X. Wang, W. Jiang, Y. Yan, T. Gong, J. Han, Z. Tian, R. Zhou, RNA viruses promote activation of the NLRP3 inflammasome through a RIP1-RIP3-DRP1 signaling pathway. *Nature immunology* **15**, 1126-1133 (2014); published online EpubOct 19 (10.1038/ni.3015).

20. W. J. Kaiser, J. W. Upton, E. S. Mocarski, Receptor-interacting protein homotypic interaction motif-dependent control of NF-kappa B activation via the DNA-dependent activator of IFN regulatory factors. *Journal of immunology* **181**, 6427-6434 (2008); published online EpubNov 1 (

21. M. Rebsamen, L. X. Heinz, E. Meylan, M. C. Michallet, K. Schroder, K. Hofmann, J. Vazquez, C. A. Benedict, J. Tschopp, DAI/ZBP1 recruits RIP1 and RIP3 through RIP homotypic interaction motifs to activate NF-kappaB. *EMBO reports* **10**, 916-922 (2009); published online EpubAug (10.1038/embor.2009.109).

22. M. Yabal, N. Muller, H. Adler, N. Knies, C. J. Gross, R. B. Damgaard, H. Kanegane, M. Ringelhan, T. Kaufmann, M. Heikenwalder, A. Strasser, O. Gross, J. Ruland, C. Peschel, M. Gyrd-Hansen, P. J. Jost, XIAP restricts TNF- and RIP3-dependent cell death and inflammasome activation. *Cell reports* **7**, 1796-1808 (2014); published online EpubJun 26 (10.1016/j.celrep.2014.05.008).

23. K. Moriwaki, J. Bertin, P. J. Gough, F. K. Chan, A RIPK3-Caspase 8 Complex Mediates Atypical Pro-IL-1beta Processing. *Journal of immunology* **194**, 1938-1944 (2015); published online EpubFeb 15 (10.4049/jimmunol.1402167).

24. K. Newton, D. L. Dugger, K. E. Wickliffe, N. Kapoor, M. C. de Almagro, D. Vucic, L. Komuves, R. E. Ferrando, D. M. French, J. Webster, M. Roose-Girma, S. Warming, V. M. Dixit, Activity of protein kinase RIPK3 determines whether cells die by necroptosis or apoptosis. *Science* **343**, 1357-1360 (2014); published online EpubMar 21 (10.1126/science.1249361).

25. P. Mandal, S. B. Berger, S. Pillay, K. Moriwaki, C. Huang, H. Guo, J. D. Lich, J. Finger, V. Kasparcova, B. Votta, M. Ouellette, B. W. King, D. Wisnoski, A. S. Lakdawala, M. P. DeMartino, L. N. Casillas, P. A. Haile, C. A. Sehon, R. W. Marquis, J. Upton, L. P. Daley-Bauer, L. Roback, N. Ramia, C. M. Dovey, J. E. Carette, F. K. Chan, J. Bertin, P. J. Gough, E. S. Mocarski, W. J. Kaiser, RIP3 induces apoptosis independent of pronecrotic kinase activity. *Molecular cell* **56**, 481-495 (2014); published online EpubNov 20 (10.1016/j.molcel.2014.10.021).

26. L. Sun, H. Wang, Z. Wang, S. He, S. Chen, D. Liao, L. Wang, J. Yan, W. Liu, X. Lei, X. Wang, Mixed lineage kinase domain-like protein mediates necrosis signaling downstream of RIP3 kinase. *Cell* **148**, 213-227 (2012); published online EpubJan 20 (10.1016/j.cell.2011.11.031).

27. J. M. Hildebrand, M. C. Tanzer, I. S. Lucet, S. N. Young, S. K. Spall, P. Sharma, C. Pierotti, J. M. Garnier, R. C. Dobson, A. I. Webb, A. Tripaydonis, J. J. Babon, M. D. Mulcair, M. J. Scanlon, W. S. Alexander, A. F. Wilks, P. E. Czabotar, G. Lessene, J. M. Murphy, J. Silke, Activation of the pseudokinase MLKL unleashes the four-helix bundle domain to induce membrane localization and necroptotic cell death. *Proceedings of the National Academy of Sciences of the United States of America* **111**, 15072-15077 (2014); published online EpubOct 21 (10.1073/pnas.1408987111).

28. J. K. Taubenberger, D. M. Morens, 1918 Influenza: the mother of all pandemics. *Emerging infectious diseases* **12**, 15-22 (2006); published online EpubJan (10.3201/eid1201.050979).

29. S. Balachandran, P. C. Roberts, T. Kipperman, K. N. Bhalla, R. W. Compans, D. R. Archer, G. N. Barber, Alpha/beta interferons potentiate virus-induced apoptosis through activation of the FADD/Caspase-8 death signaling pathway. *Journal of virology* **74**, 1513-1523 (2000); published online EpubFeb (

30. R. J. Thapa, S. Nogusa, P. Chen, J. L. Maki, A. Lerro, M. Andrake, G. F. Rall, A. Degterev, S. Balachandran, Interferon-induced RIP1/RIP3-mediated necrosis requires PKR and is licensed by FADD and caspases. *Proceedings of the National Academy of Sciences of the United States of America* **110**, E3109-3118 (2013); published online EpubAug 13 (10.1073/pnas.1301218110).

31. S. McComb, E. Cessford, N. A. Alturki, J. Joseph, B. Shutinoski, J. B. Startek, A. M. Gamero, K. L. Mossman, S. Sad, Type-I interferon signaling through ISGF3 complex is required for sustained Rip3 activation and necroptosis in macrophages. *Proceedings of the National Academy of Sciences of the United States of America* **111**, E3206-3213 (2014); published online EpubAug 5 (10.1073/pnas.1407068111).

32. S. Davidson, S. Crotta, T. M. McCabe, A. Wack, Pathogenic potential of interferon alphabeta in acute influenza infection. *Nature communications* **5**, 3864 (2014)10.1038/ncomms4864).

33. S. Nogusa, R. J. Thapa, C. P. Dillon, S. Liedmann, T. H. Oguin, 3rd, J. P. Ingram, D. A. Rodriguez, R. Kosoff, S. Sharma, O. Sturm, K. Verbist, P. J. Gough, J. Bertin, B. M. Hartmann, S. C. Sealfon, W. J. Kaiser, E. S. Mocarski, C. B. Lopez, P. G. Thomas, A. Oberst, D. R. Green, S. Balachandran, RIPK3 Activates Parallel Pathways of MLKL-Driven Necroptosis and FADD-Mediated Apoptosis to Protect against Influenza A Virus. *Cell host & microbe*, (2016); published online EpubJun 15 (10.1016/j.chom.2016.05.011).

34. J. Pothlichet, I. Meunier, B. K. Davis, J. P. Ting, E. Skamene, V. von Messling, S. M. Vidal, Type I IFN triggers RIG-I/TLR3/NLRP3-dependent inflammasome activation in influenza A virus infected cells. *PLoS pathogens* **9**, e1003256 (2013)10.1371/journal.ppat.1003256).

35. J. L. McAuley, M. D. Tate, C. J. MacKenzie-Kludas, A. Pinar, W. Zeng, A. Stutz, E. Latz, L. E. Brown, A. Mansell, Activation of the NLRP3 inflammasome by IAV virulence protein PB1-F2 contributes to severe pathophysiology and disease. *PLoS pathogens* **9**, e1003392 (2013)10.1371/journal.ppat.1003392).

36. A. Chakrabarti, S. Banerjee, L. Franchi, Y. M. Loo, M. Gale, Jr., G. Nunez, R. H. Silverman, RNase L activates the NLRP3 inflammasome during viral infections. *Cell host & microbe* **17**, 466-477 (2015); published online EpubApr 8 (10.1016/j.chom.2015.02.010).

37. W. Chen, P. A. Calvo, D. Malide, J. Gibbs, U. Schubert, I. Bacik, S. Basta, R. O'Neill, J. Schickli, P. Palese, P. Henklein, J. R. Bennink, J. W. Yewdell, A novel influenza A virus mitochondrial protein that induces cell death. *Nature medicine* **7**, 1306-1312 (2001); published online EpubDec (10.1038/nm1201-1306).

38. M. D. de Jong, C. P. Simmons, T. T. Thanh, V. M. Hien, G. J. Smith, T. N. Chau, D. M. Hoang, N. V. Chau, T. H. Khanh, V. C. Dong, P. T. Qui, B. V. Cam, Q. Ha do, Y. Guan, J. S. Peiris, N. T. Chinh, T. T. Hien, J. Farrar, Fatal outcome of human influenza A (H5N1) is associated with high viral load and hypercytokinemia. *Nature medicine* **12**, 1203-1207 (2006); published online EpubOct (10.1038/nm1477).

39. A. R. Everitt, S. Clare, T. Pertel, S. P. John, R. S. Wash, S. E. Smith, C. R. Chin, E. M. Feeley, J. S. Sims, D. J. Adams, H. M. Wise, L. Kane, D. Goulding, P. Digard, V. Anttila, J. K. Baillie, T. S. Walsh, D. A. Hume, A. Palotie, Y. Xue, V. Colonna, C. Tyler-Smith, J. Dunning, S. B. Gordon, I. I. Gen, M. Investigators, R. L. Smyth, P. J. Openshaw, G. Dougan, A. L. Brass, P. Kellam, IFITM3 restricts the morbidity and mortality associated with influenza. *Nature* **484**, 519-523 (2012); published online EpubApr 26 (10.1038/nature10921).

40. M. Brandes, F. Klauschen, S. Kuchen, R. N. Germain, A systems analysis identifies a feedforward inflammatory circuit leading to lethal influenza infection. *Cell* **154**, 197-212 (2013); published online EpubJul 3 (10.1016/j.cell.2013.06.013).

41. J. C. Kash, T. M. Tumpey, S. C. Proll, V. Carter, O. Perwitasari, M. J. Thomas, C. F. Basler, P. Palese, J. K. Taubenberger, A. Garcia-Sastre, D. E. Swayne, M. G. Katze, Genomic analysis of increased host immune and cell death responses induced by 1918 influenza virus. *Nature* **443**, 578-581 (2006); published online EpubOct 5 (10.1038/nature05181).

42. S. Li, L. Wang, M. Berman, Y. Y. Kong, M. E. Dorf, Mapping a dynamic innate immunity protein interaction network regulating type I interferon production. *Immunity* **35**, 426-440 (2011); published online EpubSep 23 (10.1016/j.immuni.2011.06.014).

43. T. H. Pham, K. M. Kwon, Y. E. Kim, K. K. Kim, J. H. Ahn, DNA sensing-independent inhibition of herpes simplex virus 1 replication by DAI/ZBP1. *Journal of virology* **87**, 3076-3086 (2013); published online EpubMar (10.1128/JVI.02860-12).

44. V. R. DeFilippis, D. Alvarado, T. Sali, S. Rothenburg, K. Fruh, Human cytomegalovirus induces the interferon response via the DNA sensor ZBP1. *Journal of virology* **84**, 585-598 (2010); published online EpubJan (10.1128/JVI.01748-09).

45. W. J. Kaiser, J. W. Upton, A. B. Long, D. Livingston-Rosanoff, L. P. Daley-Bauer, R. Hakem, T. Caspary, E. S. Mocarski, RIP3 mediates the embryonic lethality of caspase-8-deficient mice. *Nature* **471**, 368-372 (2011); published online EpubMar 17 (nature09857 [pii]10.1038/nature09857).

46. A. Oberst, C. P. Dillon, R. Weinlich, L. L. McCormick, P. Fitzgerald, C. Pop, R. Hakem, G. S. Salvesen, D. R. Green, Catalytic activity of the caspase-8-FLIP(L) complex inhibits RIPK3-dependent necrosis. *Nature* **471**, 363-367 (2011); published online EpubMar 17 (nature09852 [pii]10.1038/nature09852).

47. J. M. Murphy, P. E. Czabotar, J. M. Hildebrand, I. S. Lucet, J. G. Zhang, S. Alvarez-Diaz, R. Lewis, N. Lalaoui, D. Metcalf, A. I. Webb, S. N. Young, L. N. Varghese, G. M. Tannahill, E. C. Hatchell, I. J. Majewski, T. Okamoto, R. C. Dobson, D. J. Hilton, J. J. Babon, N. A. Nicola, A. Strasser, J. Silke, W. S. Alexander, The pseudokinase MLKL mediates necroptosis via a molecular switch mechanism. *Immunity* **39**, 443-453 (2013); published online EpubSep 19 (10.1016/j.immuni.2013.06.018).

48. N. J. Chen, Chio, II, W. J. Lin, G. Duncan, H. Chau, D. Katz, H. L. Huang, K. A. Pike, Z. Hao, Y. W. Su, K. Yamamoto, R. F. de Pooter, J. C. Zuniga-Pflucker, A. Wakeham, W. C. Yeh, T. W. Mak, Beyond tumor necrosis factor receptor: TRADD signaling in toll-like receptors. *Proceedings of the National Academy of Sciences of the United States of America* **105**, 12429-12434 (2008); published online EpubAug 26 (10.1073/pnas.0806585105).

Acknowledgments:

We thank A. Burton and D. Horn for technical support, Dr. Ken J. Ishii (Osaka University) and Dr. Vishva M. Dixit (Genentech) for supplying mutant mice, Dr. P.G. Thomas (St. Jude) for MCMV Smith MSGV strain and IAV (X31), Dr. Richard Webby (St. Jude) for seasonal strains of IAV and plasmids encoding IAV proteins, Dr. Charles Russell (St. Jude) for SeV and Dr. Michael A. Whitt (UTHSS) for VSV. Confocal microscopy images were acquired at the St. Jude Cell & Tissue Imaging Center, which is supported by St. Jude Children's Research Hospital and NCI P30 CA021765-35. We thank Dr. Prajwal Gurung for critical reading of the manuscript and members of the Kanneganti lab for their comments and suggestions.

Funding:

T.D.K is supported by the US National Institutes of Health (AI101935, AI124346, AR056296 and CA163507) and the American Lebanese Syrian Associated Charities; S.M.M is supported by the National health & Medical Research Council of Australia R.G. Menzies Early Career Fellowship.

Authors Contributions:

T.K. and T.D.K. conceptualized the study; T.K., R.K.S.M., K.S., S.M.M., R.K., D.P., G.N designed the methodology, performed the experiments and conducted the analysis; P.V. performed histopathological analysis; T.K. performed statistical analysis; T.K., S.M.M., and T.D.K. wrote the manuscript; T.D.K. acquired the funding and provided overall supervision.

Competing financial interests:

The authors declare no competing financial interests.

Data and material availability:

The microarray dataset was deposited under the accession code GSE77611.

Figure Legends

Figure 1. The IFN-inducible protein ZBP1 mediates cell death in response to IAV infection. (A and B) Microscopic analysis and quantification of cell death by LDH release in BMDMs infected with IAV 16 h pi (p= 0.0131; paired *t* test; n=4). **(C and D)** Microscopic analysis and quantification of cell death by LDH release in ear fibroblasts infected with IAV 16 h pi (p= $2.92096*10^{-6}$; paired *t* test; n=4). **(E)** Microarray gene expression dataset enriched for nucleic acid sensing pathways with higher or lower expression in WT and *Ifnar1*$^{-/-}$ BMDMs 9 h pi with IAV (one experiment with two biological replicates per genotype). **(F)** Real-time quantitative RT-PCR analysis of *Zbp1* expression in WT and *Ifnar1*$^{-/-}$ BMDMs 9 h pi with IAV (one experiment with two biological replicates per genotype). **(G)** Immunoblot analysis of ZBP1 and GAPDH (loading control) in unprimed BMDMs (0-12) h pi with IAV (n=3). **(H)** Immunostaining for ZBP1 in WT BMDMs infected with IAV for 16 h (n=2). **(I and J)** Microscopic analysis and quantification of cell death by LDH release in BMDMs infected with IAV 16 h pi (p= 0.0001; one-way ANOVA; n=5). **(K and L)** Microscopic analysis and quantification of cell death by LDH release in fibroblasts infected with IAV 16 h pi (p= 0.000460657; paired *t* test; n=3). **(M)** Real time analysis of the kinetics of cell death in primary ear fibroblasts infected with IAV (MOI, 10) (one experiment with three biological replicates per genotype).

Figure 2. ZBP1 regulates NLRP3 inflammasome activation and proinflammatory cytokine production during IAV infection. (A) Immunoblot analysis of pro-caspase-1 and caspase-1 subunit p20 in BMDMs 16 h pi with IAV (n=4). **(B and C)** Levels of IL-1β

and IL-18 in cell culture supernatants 16 h pi with IAV; p= 0.0007 (IL-1β); p = 0.0015 (IL-18) one-way ANOVA; n=3). **(D and E)** Immunoblot analysis of pro-caspase-1 and caspase-1 subunit p20 in BMDMs 16 h pi with VSV or IAV (n=3). **(F)** Immunoprecipitation of ZBP1 from lysates of WT BMDMs infected with IAV for 16 h, and immunoblotted for ZBP1 and RIPK3 (n=3). **(G)** Immunoblot analysis of pro-caspase-1 and caspase-1 subunit p20 inBMDMs 16 h pi with IAV (n=3). **(H)** Levels of IL-1β and IL-18 in cell culture supernatants 16 h pi with IAV; p=0.0003 (IL-1β); p=0.0033 (IL-18); one-way ANOVA; n=3). **(I and J)** Levels of TNF and IL-6 in cell culture supernatants 16 h pi with IAV. **(I)** p=0.0003 (IL-6; one way ANOVA); p=0.04585299 (TNF; paired *t* test); n=3 **(J)** p=0.00427068 (IL-6; paired t-test); p=0.01547619 (TNF; paired *t* test); n=3).

Figure 3. ZBP1 mediates induction of apoptotic and necroptotic cell death pathways during IAV infection via RIPK3. (A and B) Microscopic analysis and quantification of cell death by LDH release in fibroblasts infected with IAV 16 h pi; p=0.0016; one-way ANOVA; n=3. **(C)** Quantification of cell death by LDH release in BMDMs infected with IAV 16 h pi (p=0.0001; one-way ANOVA; n=4). **(D)** Immunoblot analysis of the pro- and cleaved-forms of caspase-8, caspase-3 and caspase-7 in BMDMs 16 h pi with IAV (n=3). **(E)** Microscopic analysis of BMDMs infected with IAV for 16 h in the absence or presence of inhibitors (n=3).

Figure 4. ZBP1 regulates cell death in response to both mouse-adapted and human strains of IAV, but not in response to other RNA viruses.

(A to F) Microscopic analysis and quantification of cell death by LDH release in fibroblasts infected with mouse adapted Influenza A/X31 (H3N2), Influenza A/Brisbane/59/2007 (H1N1) and A/Switzerland/9715293/2013 (H3N2) after 16 h (p=

4.5184*10^{-5} (X31); p=0.02523 (A/Brisbane); p=0.00671454 (A/Switzerland); paired *t* test; n=4) **(G)** Quantification of cell death by LDH release in BMDMs infected with VSV (MOI 10), SeV (MOI,8) and RSV (MOI10) 16 h pi (n=3).

Figure 5. ZBP1 functions as a sensor of IAV infection by interacting with IAV PB1 and NP proteins. (**A**) Immunoprecipitation of endogenous ZBP1 from lysates of WT BMDMs infected with IAV for 16 h, and immunoblotted for ZBP1, M1, NS1 and HA; n=. **(B)** Immunoprecipitation of endogenous ZBP1 from lysates of WT or *Zbp1*$^{-/-}$ fibroblasts infected with IAV for 16 h, and immunoblotted for ZBP1, PB1 and NP; n=. **(C)** Immunoprecipitation of ZBP1, PB1 and NP from lysates of WT fibroblasts infected with IAV for 16 h, and immunoblotted for ZBP1, PB1 and NP; n=. **(D)** Immunoblot analysis of ZBP1, PB1, NP and GAPDH from whole cell lysates, nuclear and cytoplasmic fractions of WT fibroblasts infected with IAV for 8 h; n=3. **(E)** Immunoprecipitation of HA-tagged ZBP1 from lysates of 239T cells expressing HA-tagged ZBP1 transfected with plasmids expressing PB1 or NP, and immunoblotted for ZBP1, PB1 and NP; n=. **(F)** Domain architecture of murine ZBP1 and schematics of the constructs used in this study. **(G and H)** Immunoprecipitation of HA-tagged ZBP1 from lysates of 239T cells expressing HA-tagged ZBP1 constructs infected with IAV for 16 h, and immunoblotted for the IAV proteins PB1, HA and NP, and HA tag; n=.

Figure 6. ZBP1 promotes inflammatory responses and epithelial damage during IAV infection *in vivo*. **(A)** Survival analysis of female WT and *Zbp1*$^{-/-}$ mice infected with one LD_{50} of IAV; p=0.0819; Mantel-Cox test; n = 13 WT and 9 *Zbp1*$^{-/-}$ mice. **(B)** Body weight of WT (n = 21) and *Zbp1*$^{-/-}$ (n = 15) mice 0–18 d after infection; p=0.02743813 (D5); 0.00103121 (D6); 0.00081354 (D7); 0.05424982 (D14); 0.0231683 (D15);

0.02152296 (D16); two-tailed *t* test. **(C)** Lung viral titers in WT and *Zbp1*$^{-/-}$ mice infected with IAV for 7 days; p=6.23229*10^{-5}; two-tailed *t* test; n=6. H &E staining **(D)** and immunohistochemistry analysis for IAV NP protein **(E)** of lungs from WT and *Zbp1*$^{-/-}$ mice infected with IAV for 7 days; n=6.

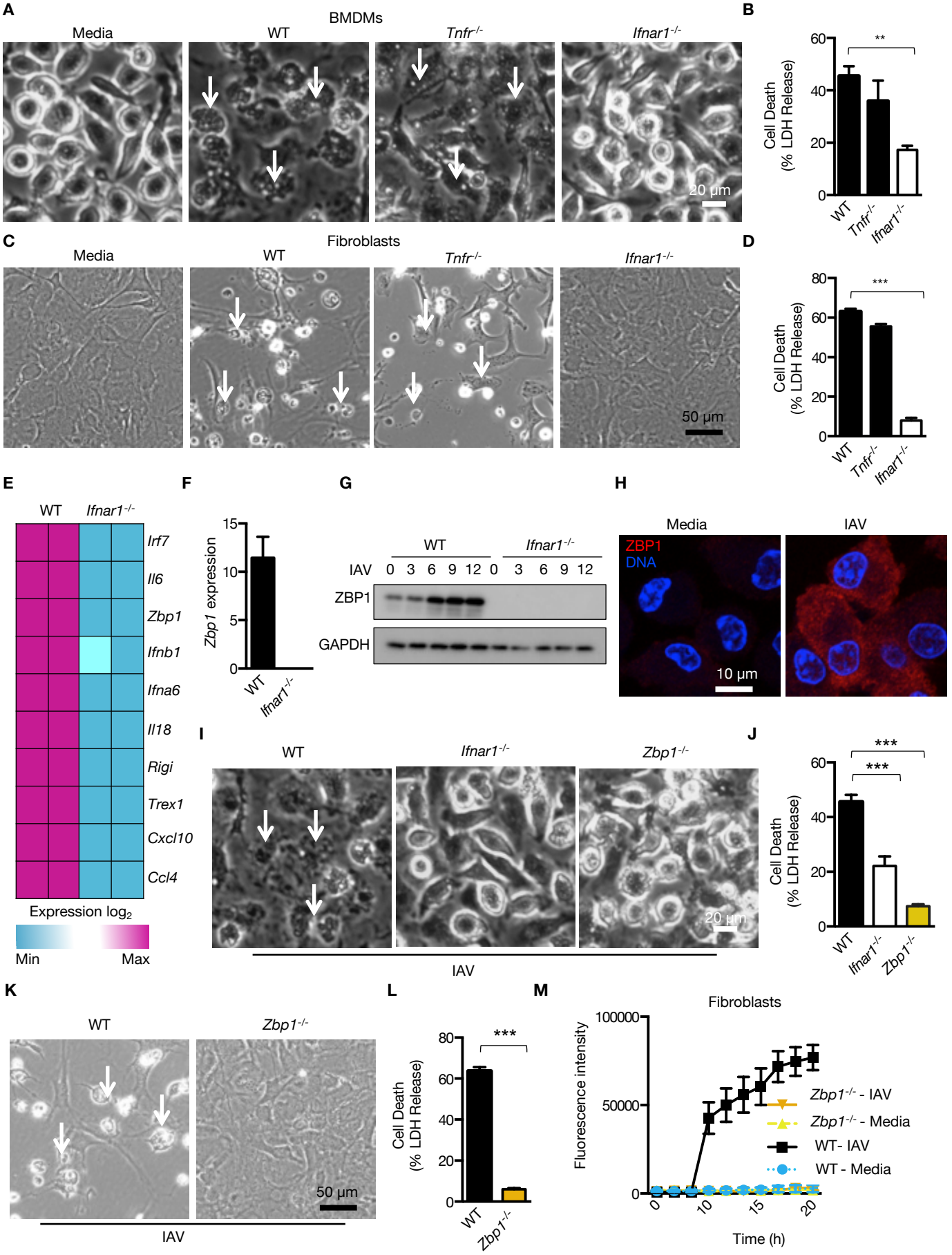
A
BMDMs
Media
WT
Tnfr-/-
Ifnar1-/-
20 μm
B
Cell Death (% LDH Release)
**
WT
Tnfr-/-
Ifnar1-/-
C
Fibroblasts
Media
WT
Tnfr-/-
Ifnar1-/-
50 μm
D
Cell Death (% LDH Release)
***
WT
Tnfr-/-
Ifnar1-/-
E
WT
Ifnar1-/-
Irf7
Il6
Zbp1
Ifnb1
Ifna6
Il18
Rigi
Trex1
Cxcl10
Ccl4
Expression log2
Min
Max
F
Zbp1 expression
WT
Ifnar1-/-
G
WT
Ifnar1-/-
IAV 0 3 6 9 12 0 3 6 9 12
ZBP1
GAPDH
H
Media
IAV
ZBP1
DNA
10 μm
I
WT
Ifnar1-/-
Zbp1-/-
20 μm
IAV
J
***
***
Cell Death (% LDH Release)
WT
Ifnar1-/-
Zbp1-/-
K
WT
Zbp1-/-
50 μm
IAV
L
***
Cell Death (% LDH Release)
WT
Zbp1-/-
M
Fibroblasts
Fluorescence intensity
Zbp1-/- - IAV
Zbp1-/- - Media
WT- IAV
WT - Media
Time (h)

Figure 1

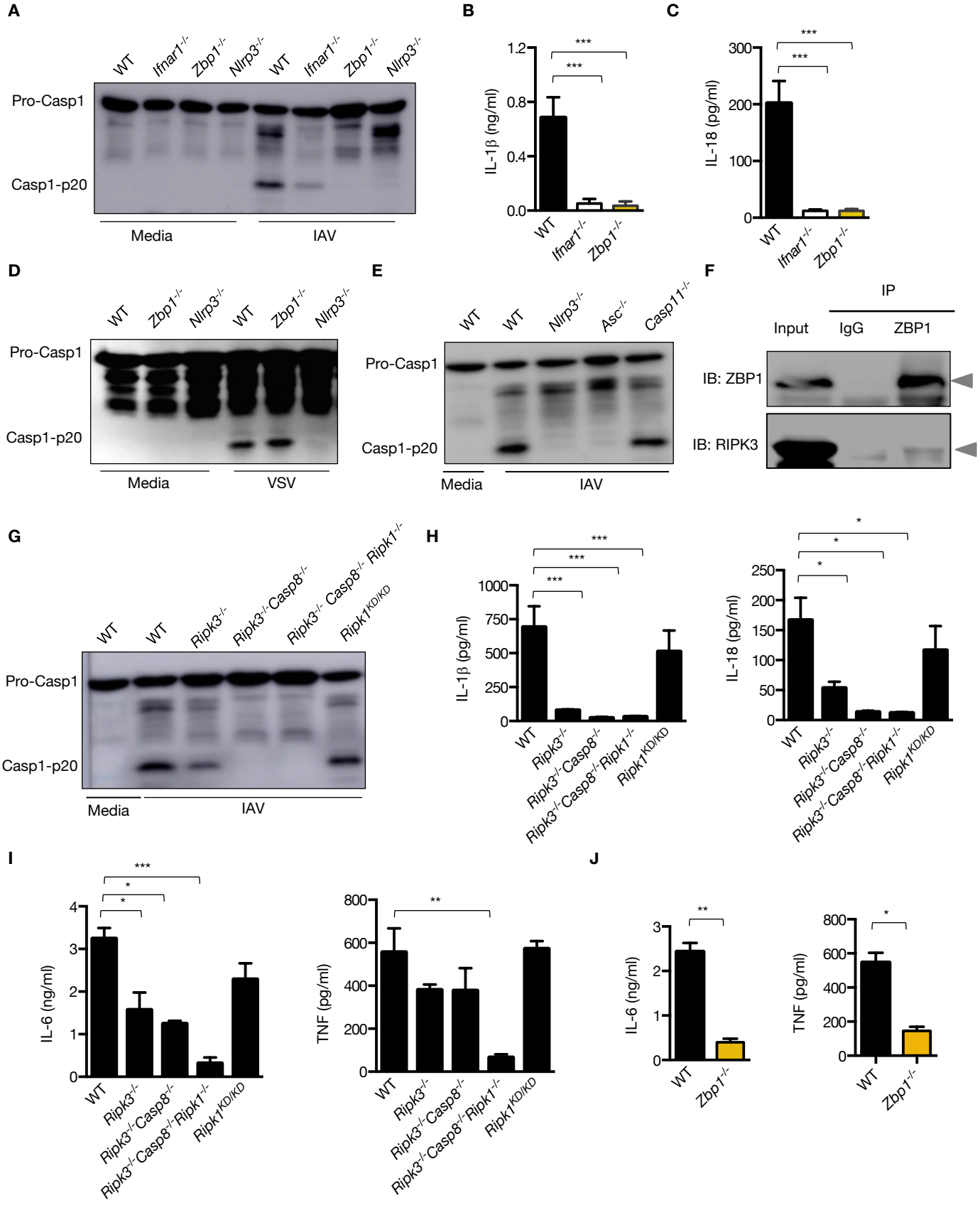
A
WT
Ifnar1-/-
Zbp1-/-
Nlrp3-/-
WT
Ifnar1-/-
Zbp1-/-
Nlrp3-/-
Pro-Casp1
Casp1-p20
Media
IAV
B
IL-1β (ng/ml)
***
***
WT
Ifnar1-/-
Zbp1-/-
C
IL-18 (pg/ml)
***
***
WT
Ifnar1-/-
Zbp1-/-
D
WT
Zbp1-/-
Nlrp3-/-
WT
Zbp1-/-
Nlrp3-/-
Pro-Casp1
Casp1-p20
Media
VSV
E
WT
WT
Nlrp3-/-
Asc-/-
Casp11-/-
Pro-Casp1
Casp1-p20
Media
IAV
F
IP
Input
IgG
ZBP1
IB: ZBP1
IB: RIPK3
G
WT
WT
Ripk3-/-
Ripk3-/-Casp8-/-
Ripk3-/- Casp8-/- Ripk1-/-
Ripk1KD/KD
Pro-Casp1
Casp1-p20
Media
IAV
H
IL-1β (pg/ml)
***
***
***
WT
Ripk3-/-
Ripk3-/-Casp8-/-
Ripk3-/-Casp8-/-Ripk1-/-
Ripk1KD/KD
IL-18 (pg/ml)
*
*
*
WT
Ripk3-/-
Ripk3-/-Casp8-/-
Ripk3-/-Casp8-/-Ripk1-/-
Ripk1KD/KD
I
IL-6 (ng/ml)
***
*
*
WT
Ripk3-/-
Ripk3-/-Casp8-/-
Ripk3-/-Casp8-/-Ripk1-/-
Ripk1KD/KD
TNF (pg/ml)
**
WT
Ripk3-/-
Ripk3-/-Casp8-/-
Ripk3-/-Casp8-/-Ripk1-/-
Ripk1KD/KD
J
IL-6 (ng/ml)
**
WT
Zbp1-/-
TNF (pg/ml)
*
WT
Zbp1-/-

Figure 2

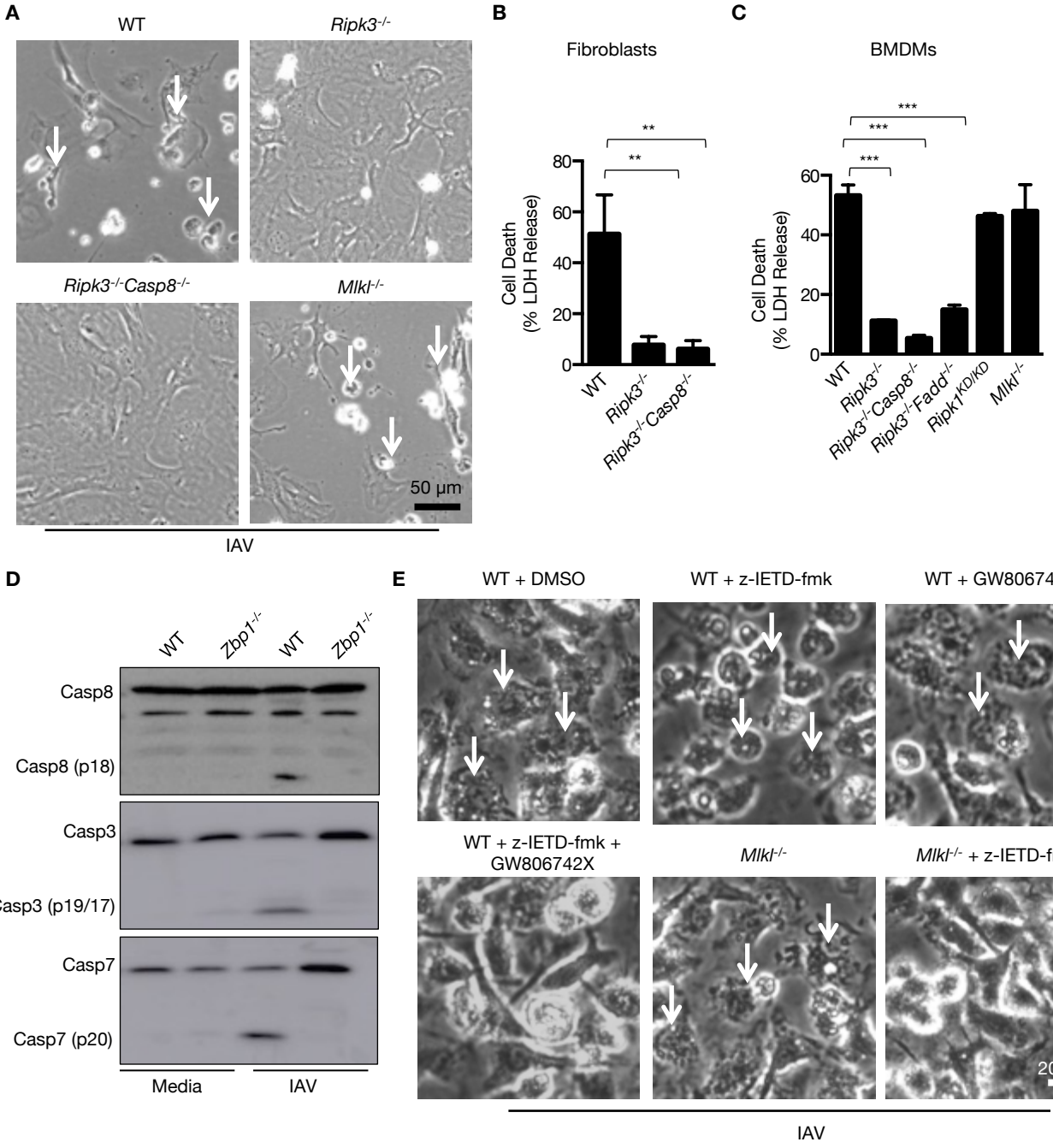
A
WT
Ripk3-/-
Ripk3-/-Casp8-/-
Mlkl-/-
50 μm
IAV
B
Fibroblasts
Cell Death (% LDH Release)
WT
Ripk3-/-
Ripk3-/-Casp8-/-
C
BMDMs
Cell Death (% LDH Release)
WT
Ripk3-/-
Ripk3-/-Casp8-/-
Ripk3-/-Fadd-/-
Ripk1KDIKD
Mlkl-/-
D
WT
Zbp1-/-
WT
Zbp1-/-
Casp8
Casp8 (p18)
Casp3
Casp3 (p19/17)
Casp7
Casp7 (p20)
Media
IAV
E
WT + DMSO
WT + z-IETD-fmk
WT + GW806742X
WT + z-IETD-fmk + GW806742X
Mlkl-/-
Mlkl-/- + z-IETD-fmk
20 μm
IAV

Figure 3

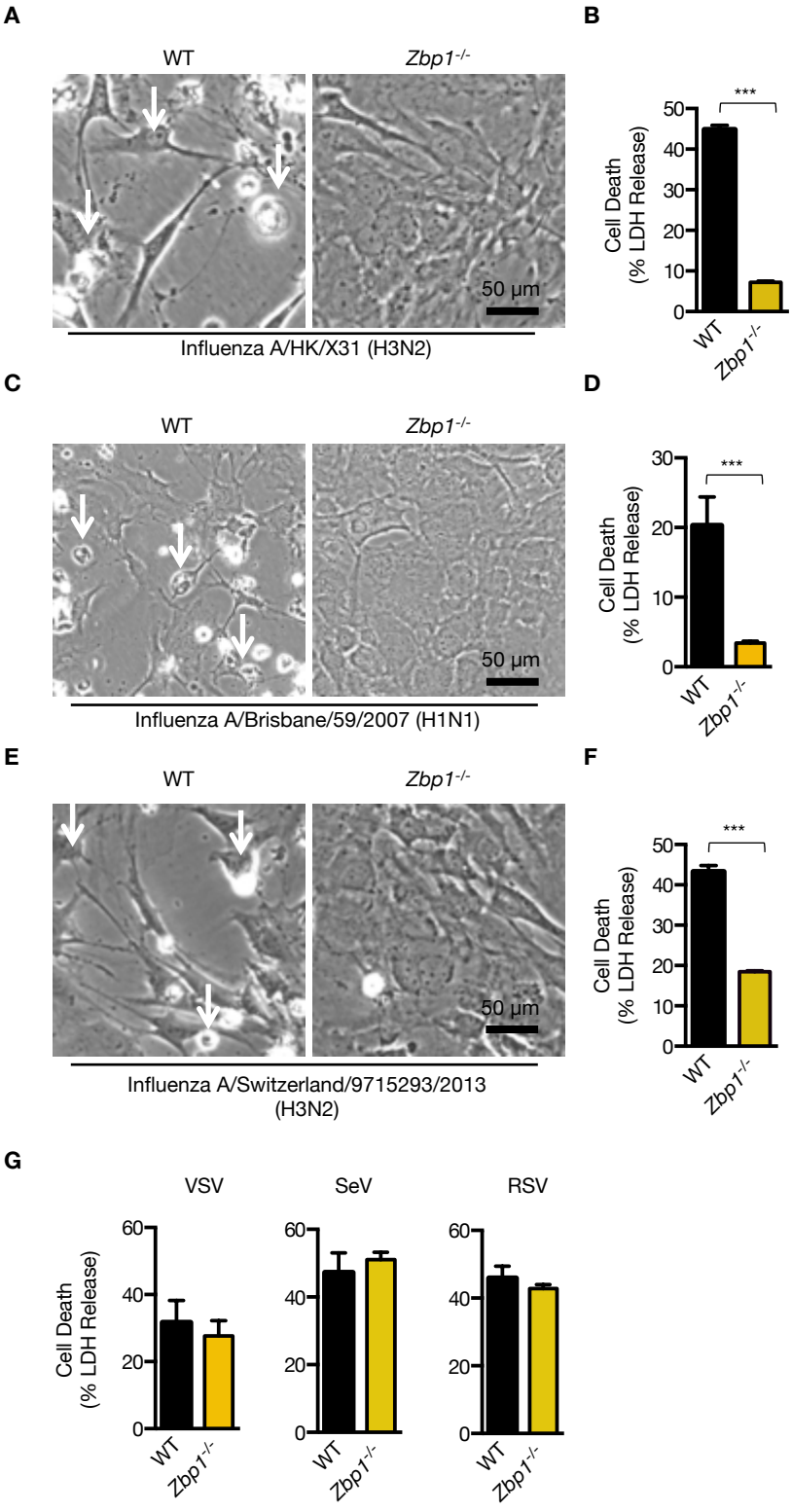
A
WT
Zbp1-/-
50 μm
Influenza A/HK/X31 (H3N2)
B
***
Cell Death
(% LDH Release)
50
40
30
20
10
0
WT
Zbp1-/-
C
WT
Zbp1-/-
50 μm
Influenza A/Brisbane/59/2007 (H1N1)
D
***
Cell Death
(% LDH Release)
30
20
10
0
WT
Zbp1-/-
E
WT
Zbp1-/-
50 μm
Influenza A/Switzerland/9715293/2013
(H3N2)
F
***
Cell Death
(% LDH Release)
50
40
30
20
10
0
WT
Zbp1-/-
G
VSV
SeV
RSV
Cell Death
(% LDH Release)
60
40
20
0
WT
Zbp1-/-

Figure 4

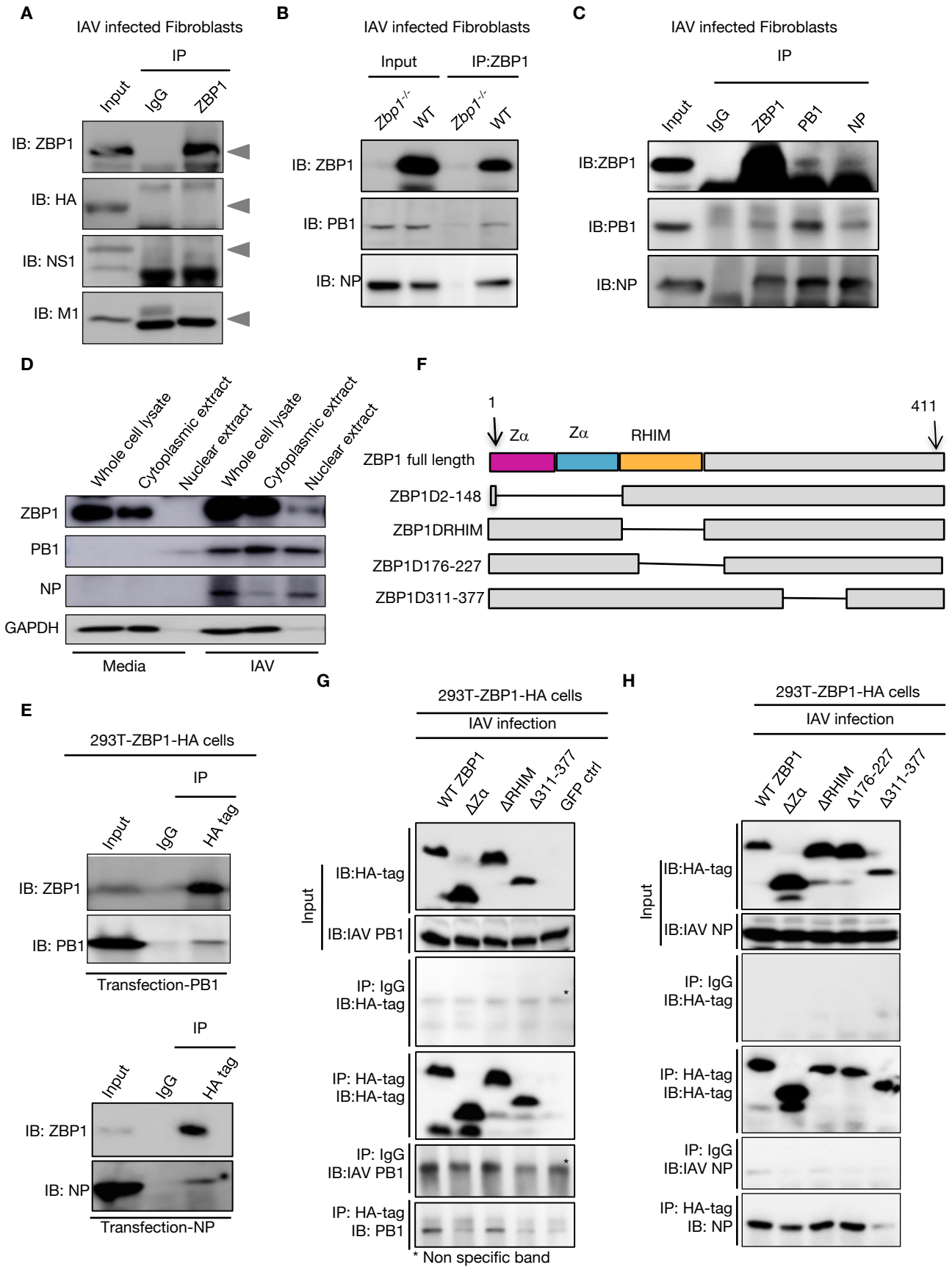
A
IAV infected Fibroblasts
IP
Input
IgG
ZBP1
IB: ZBP1
IB: HA
IB: NS1
IB: M1
B
IAV infected Fibroblasts
Input
IP:ZBP1
Zbp1-/-
WT
Zbp1-/-
WT
IB: ZBP1
IB: PB1
IB: NP
C
IAV infected Fibroblasts
IP
Input
IgG
ZBP1
PB1
NP
IB:ZBP1
IB:PB1
IB:NP
D
Whole cell lysate
Cytoplasmic extract
Nuclear extract
Whole cell lysate
Cytoplasmic extract
Nuclear extract
ZBP1
PB1
NP
GAPDH
Media
IAV
F
1
411
Zα
Zα
RHIM
ZBP1 full length
ZBP1D2-148
ZBP1DRHIM
ZBP1D176-227
ZBP1D311-377
E
293T-ZBP1-HA cells
IP
Input
IgG
HA tag
IB: ZBP1
IB: PB1
Transfection-PB1
IP
Input
IgG
HA tag
IB: ZBP1
IB: NP
Transfection-NP
G
293T-ZBP1-HA cells
IAV infection
WT ZBP1
ΔZα
ΔRHIM
Δ311-377
GFP ctrl
Input
IB:HA-tag
IB:IAV PB1
IP: IgG
IB:HA-tag
IP: HA-tag
IB:HA-tag
IP: IgG
IB:IAV PB1
IP: HA-tag
IB: PB1
* Non specific band
H
293T-ZBP1-HA cells
IAV infection
WT ZBP1
ΔZα
ΔRHIM
Δ176-227
Δ311-377
Input
IB:HA-tag
IB:IAV NP
IP: IgG
IB:HA-tag
IP: HA-tag
IB:HA-tag
IP: IgG
IB:IAV NP
IP: HA-tag
IB: NP

Figure 5

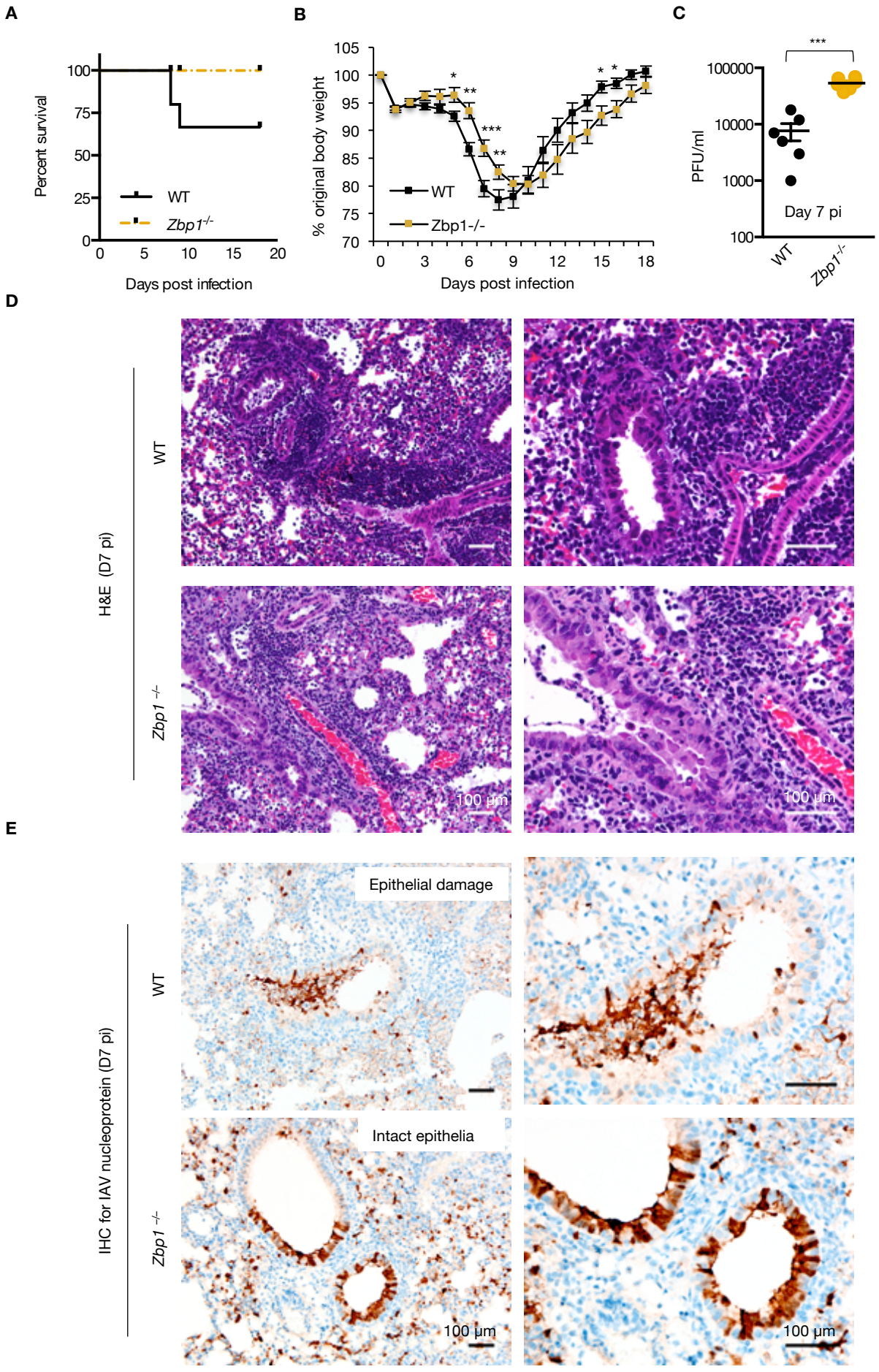
A
Percent survival
100
75
50
25
0
0
5
10
15
20
Days post infection
WT
Zbp1-/-
B
% original body weight
105
100
95
90
85
80
75
70
0
3
6
9
12
15
18
Days post infection
WT
Zbp1-/-
C
PFU/ml
100000
10000
1000
100
***
Day 7 pi
WT
Zbp1-/-
D
H&E (D7 pi)
WT
Zbp1 -/-
100 µm
100 µm
E
IHC for IAV nucleoprotein (D7 pi)
WT
Zbp1 -/-
Epithelial damage
Intact epithelia
100 µm
100 µm

Figure 6

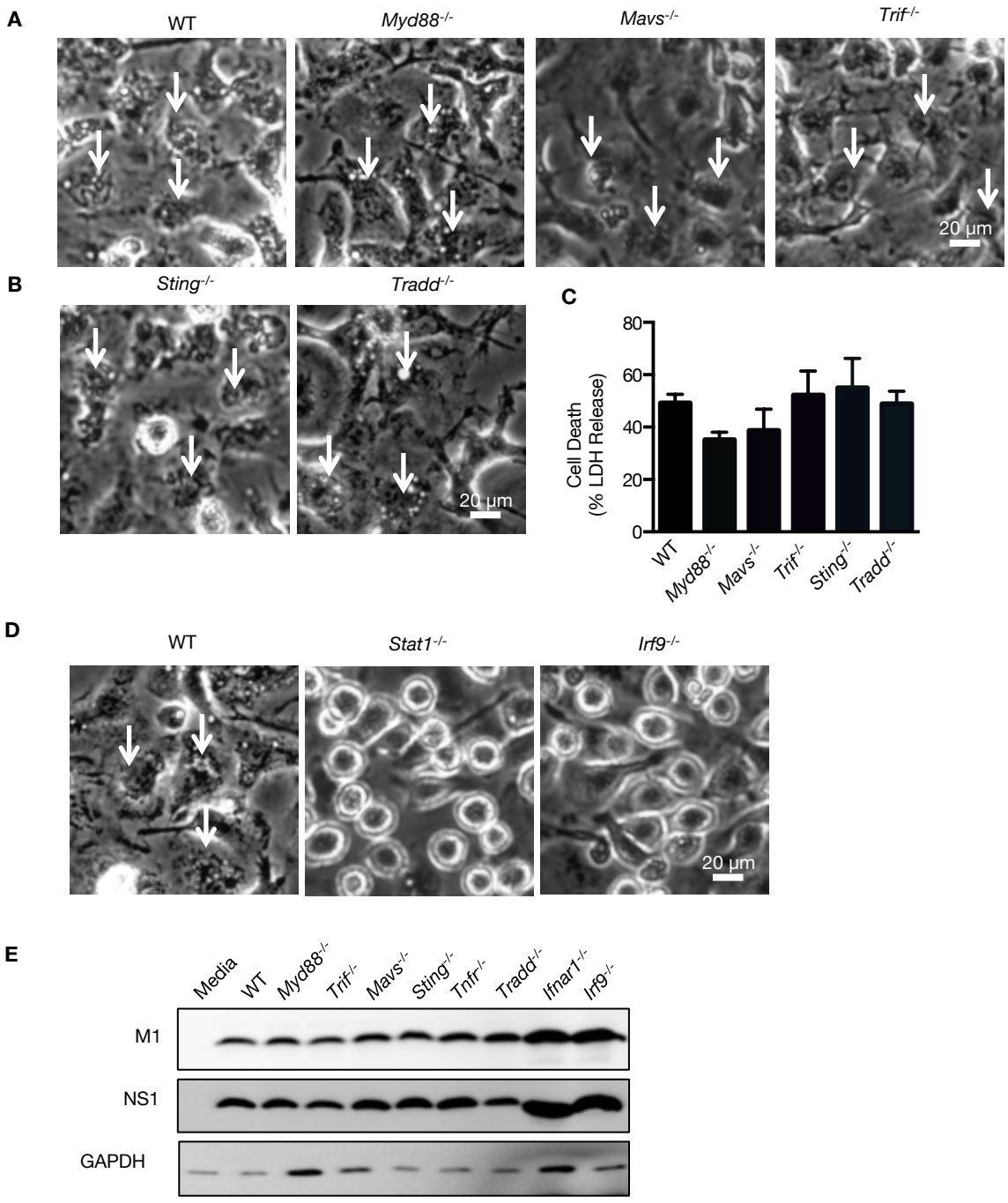
A
WT
Myd88-/-
Mavs-/-
Trif-/-
20 μm
B
Sting-/-
Tradd-/-
20 μm
C
Cell Death (% LDH Release)
80
60
40
20
0
WT
Myd88-/-
Mavs-/-
Trif-/-
Sting-/-
Tradd-/-
D
WT
Stat1-/-
Irf9-/-
20 μm
E
Media
WT
Myd88-/-
Trif-/-
Mavs-/-
Sting-/-
Tnfr-/-
Tradd-/-
Ifnar1-/-
Irf9-/-
M1
NS1
GAPDH

Fig. S1

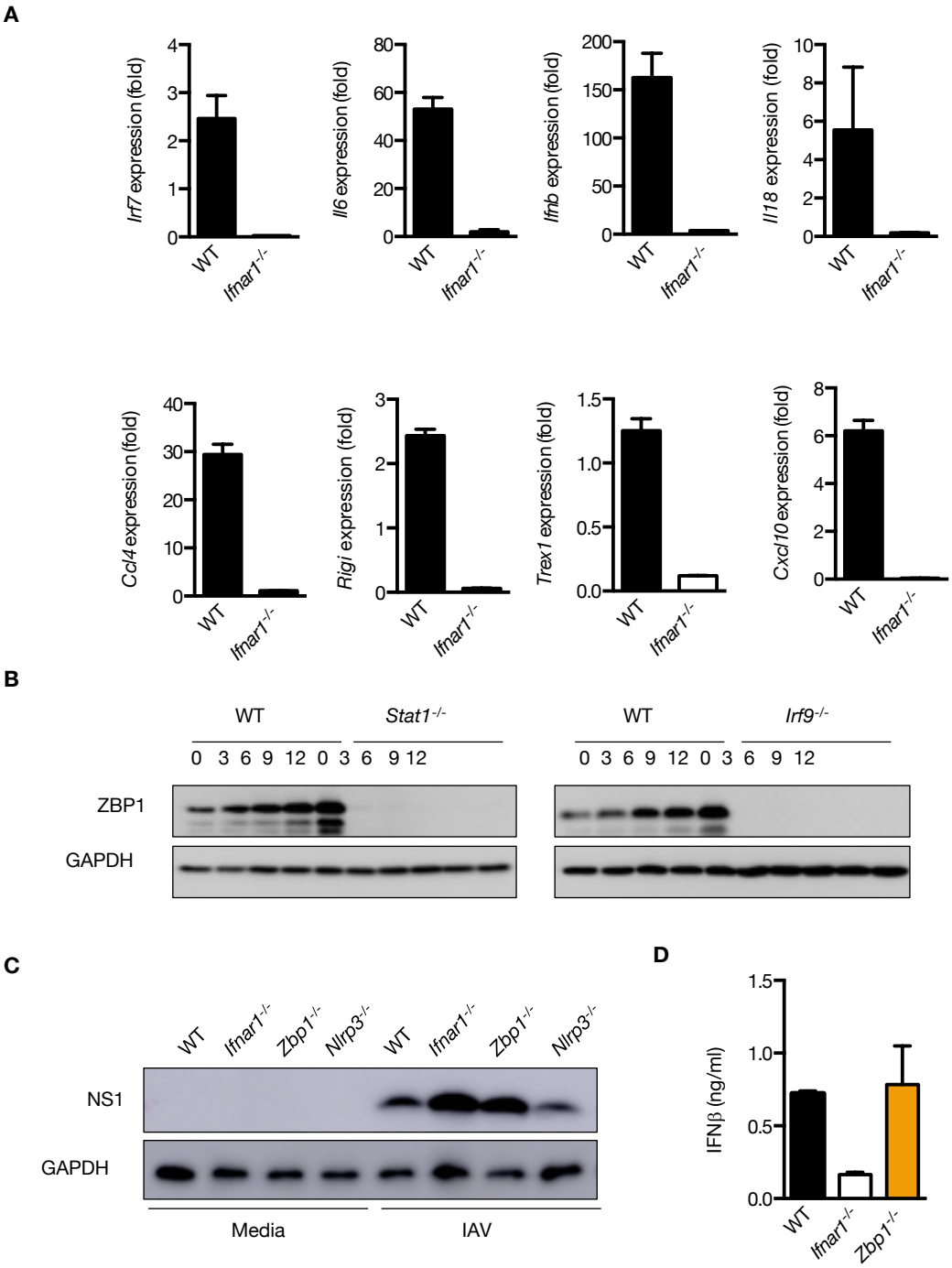
A
Irf7 expression (fold)
Il6 expression (fold)
Ifnb expression (fold)
Il18 expression (fold)
Ccl4 expression (fold)
Rigi expression (fold)
Trex1 expression (fold)
Cxcl10 expression (fold)
WT
Ifnar1-/-
B
WT
Stat1-/-
Irf9-/-
0 3 6 9 12 0 3 6 9 12
ZBP1
GAPDH
C
WT
Ifnar1-/-
Zbp1-/-
Nlrp3-/-
NS1
GAPDH
Media
IAV
D
IFNβ (ng/ml)

Fig. S2

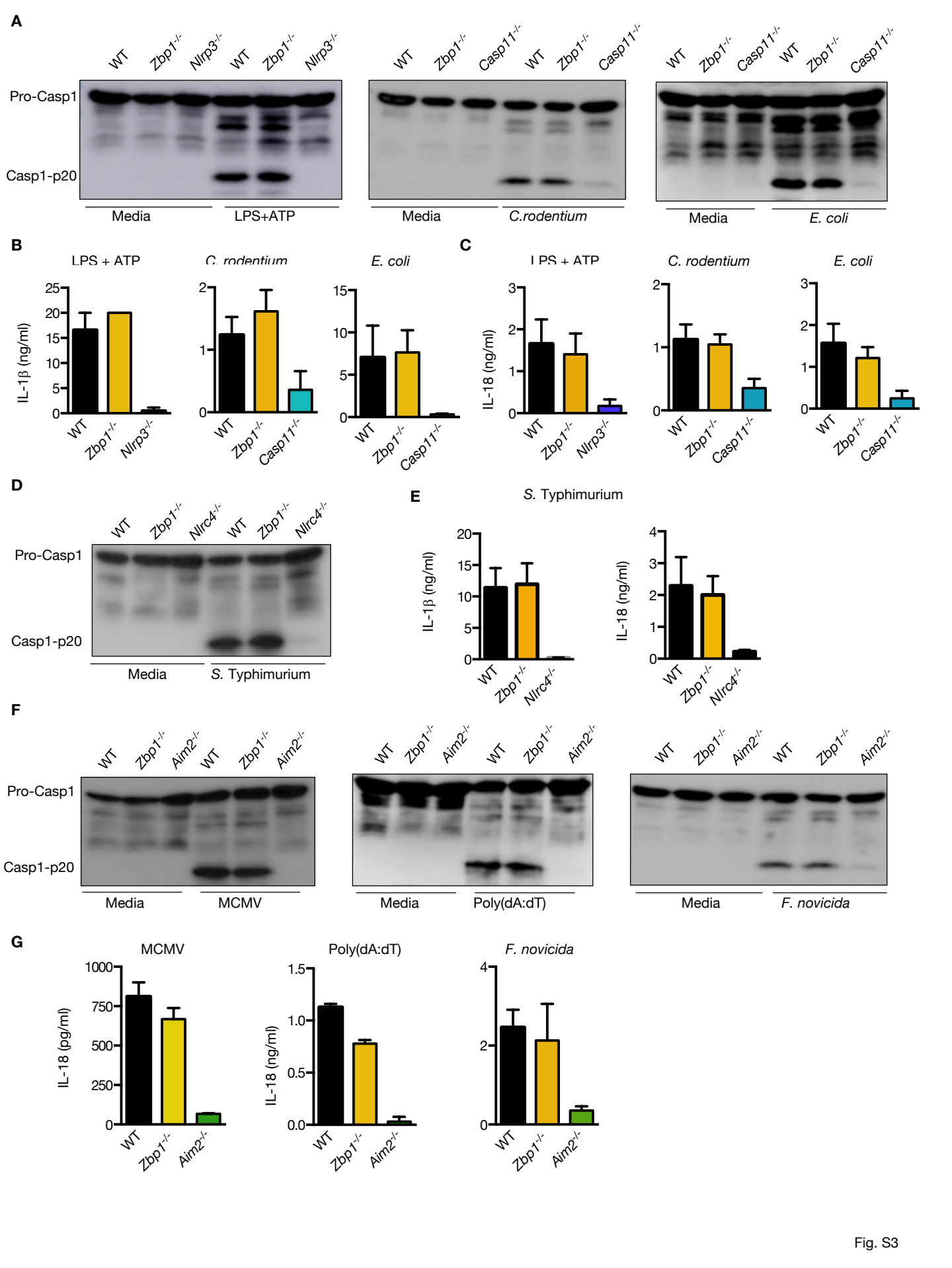
A
WT
Zbp1-/-
Nlrp3-/-
Casp11-/-
Pro-Casp1
Casp1-p20
Media
LPS+ATP
C.rodentium
E. coli
B
LPS + ATP
C. rodentium
E. coli
IL-1β (ng/ml)
C
IL-18 (ng/ml)
D
Nlrc4-/-
S. Typhimurium
E
F
Aim2-/-
MCMV
Poly(dA:dT)
F. novicida
G
IL-18 (pg/ml)

Fig. S3

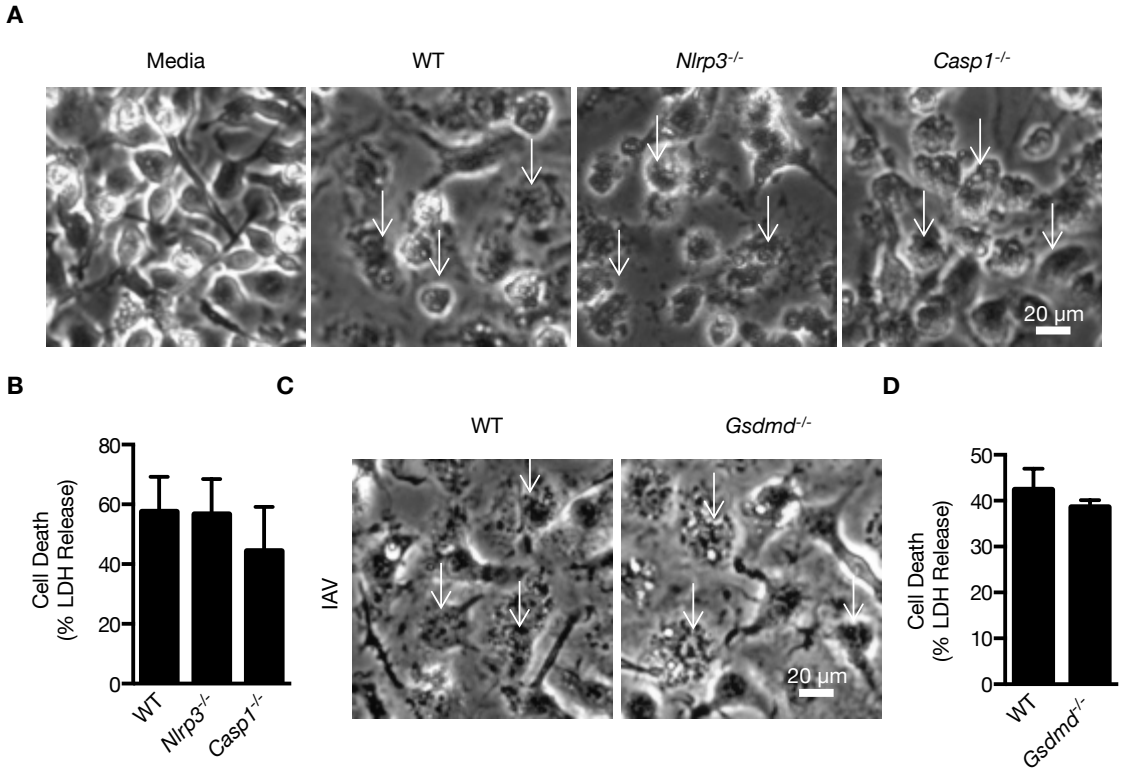
A
Media
WT
Nlrp3-/-
Casp1-/-
20 μm
B
Cell Death
(% LDH Release)
80
60
40
20
0
WT
Nlrp3-/-
Casp1-/-
C
WT
Gsdmd-/-
IAV
20 μm
D
Cell Death
(% LDH Release)
50
40
30
20
10
0
WT
Gsdmd-/-

Fig. S4

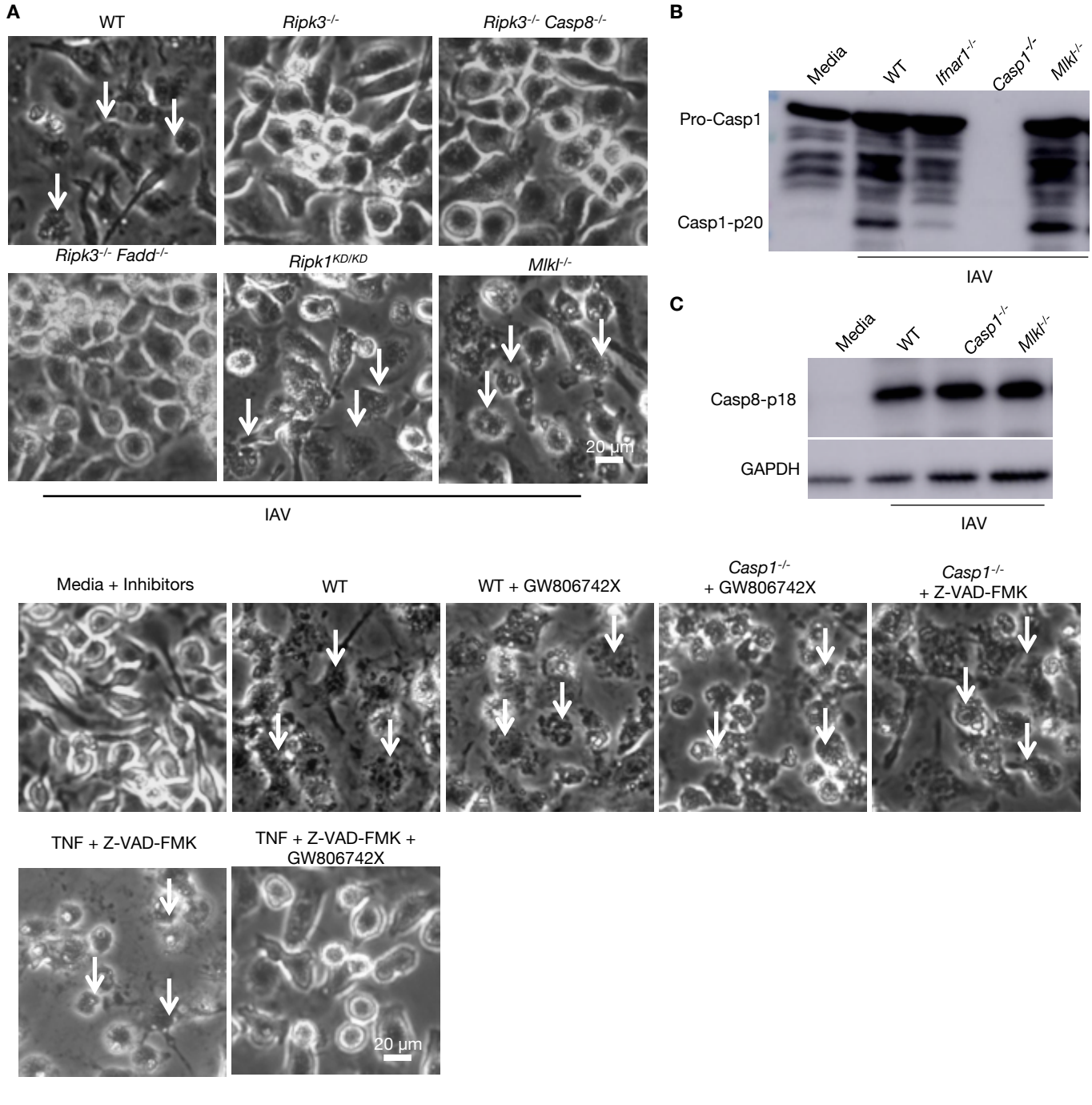
A
WT
Ripk3-/-
Ripk3-/- Casp8-/-
Ripk3-/- Fadd-/-
Ripk1KD/KD
Mlkl-/-
20 μm
IAV
B
Media
WT
Ifnar1-/-
Casp1-/-
Mlkl-/-
Pro-Casp1
Casp1-p20
IAV
C
Media
WT
Casp1-/-
Mlkl-/-
Casp8-p18
GAPDH
IAV
D
Media + Inhibitors
WT
WT + GW806742X
Casp1-/- + GW806742X
Casp1-/- + Z-VAD-FMK
TNF + Z-VAD-FMK
TNF + Z-VAD-FMK + GW806742X
20 μm

Fig. S5

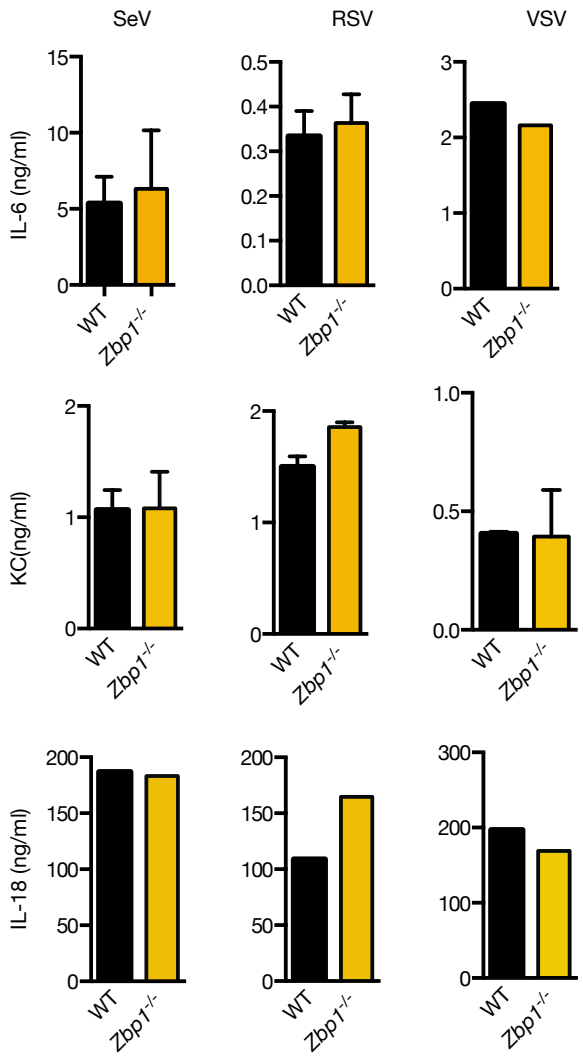

Fig. S6

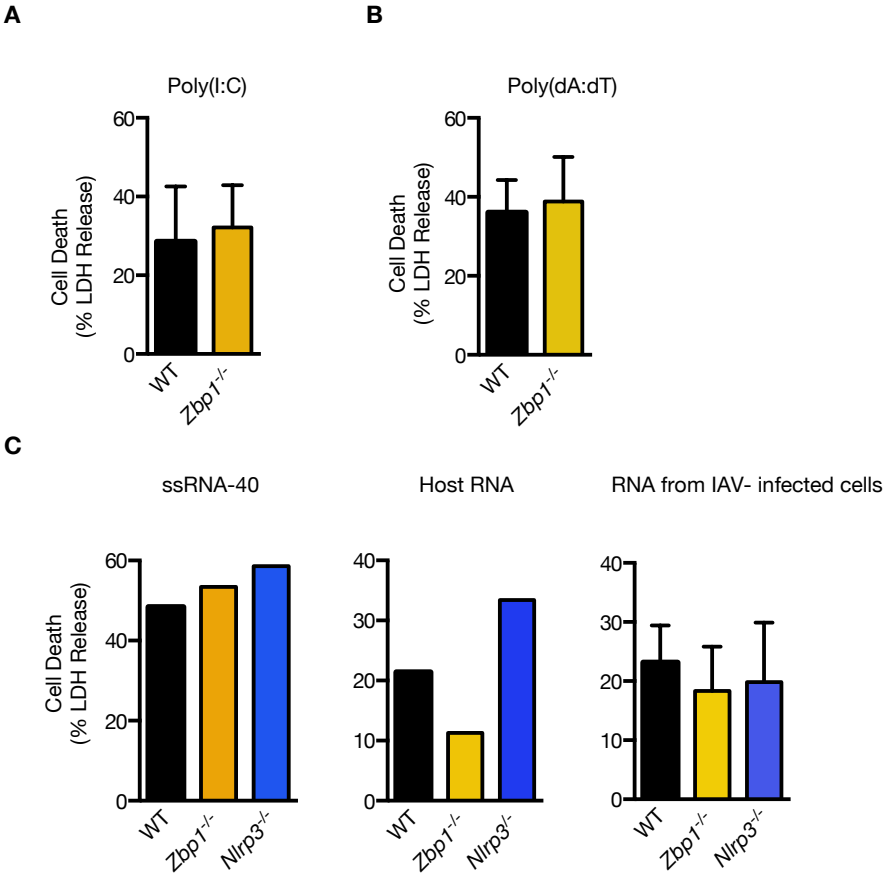
A
Poly(I:C)
Cell Death
(% LDH Release)
60
40
20
0
WT
Zbp1-/-
B
Poly(dA:dT)
Cell Death
(% LDH Release)
60
40
20
0
WT
Zbp1-/-
C
ssRNA-40
Cell Death
(% LDH Release)
60
40
20
0
WT
Zbp1-/-
Nlrp3-/-
Host RNA
40
30
20
10
0
WT
Zbp1-/-
Nlrp3-/-
RNA from IAV- infected cells
40
30
20
10
0
WT
Zbp1-/-
Nlrp3-/-

Fig. S7